Table 2
Toxicities in early phase.

	Porta hepatis group Grade					Non-porta hepatis group Grade				
	0	1	2	3	4	0	1	2	3	4
Liver	2	4	9	3	0	7	15	16	8	0
Blood	6	2	4	6	0	13	9	16	8	0

There were no significant differences between porta hepatis and non-porta hepatis groups in liver and blood toxicities (grade 0–2 vs. grade 3–4) by Fisher's exact test. $P > 0.999$ (liver toxicity); $P = 0.190$ (blood toxicity).

Table 3
Change of Child-Pugh score in late phase.

	≦1	≧2
Porta hepatis group	13	5
Non-porta hepatis group	41	5

There were no significant differences between porta hepatis and non-porta hepatis groups in change of Child-Pugh score (≦1 vs. ≧2) by Fisher's exact test. $P = 0.128$.

Discussion

It is important that the treatment of HCC involves minimum invasiveness and complications in general. Surgical resection and RFA are essential curative therapies for HCC. In surgical resection, it was reported that both the 5-year overall survival and disease-free survival rates of the anatomic resection group were significantly better than those of the non-anatomic resection group, as HCC has a nature to cause intrahepatic metastasis via vascular invasion [36]. Anatomic resection consists of the systematic removal of a hepatic segment confined by tumor-bearing portal tributaries. In some patients with HCC adjacent to the porta hepatis, anatomic resection implies greater invasiveness because the resection volume becomes larger.

Concerning the use of RFA, puncture of the liver hilus, with the risk of injury to the portal vein or bile duct, presents a potentially dangerous scenario. It was reported that RFA was performed for patients with HCC adjacent to the porta hepatis under the condition of cooling the bile duct by endoscopic nasobiliary drainage tube to prevent biliary complications [31]. But the procedure is too complex to be a common therapy. Additionally, in cases of HCC with contiguous vessels, blood flow reduces the thermal effects of RFA, a phenomenon that increases the likelihood of the presence of residual viable tumor cells [37–39].

According to the above, we need to consider the degree of invasiveness and complications and carefully select an appropriate treatment modality because HCC adjacent to the porta hepatis is close to vessels and bile duct. In this study, therefore, differences in treatment effect and toxicities according to tumor localization, whether adjacent to the porta hepatis or not, were investigated retrospectively.

In the comparison of patient and tumor characteristics, the porta hepatis group demonstrated a trend towards a higher rate of vascular invasion compared to the non-porta hepatis group ($P = 0.066$). It is suggested that this was due to the tumor location.

Local control rates after 5 years were 87.8% [95% CI, 72–104] in the porta hepatis group and 95.7% [95% CI, 90–102] in the non-porta hepatis group. Thus, we obtained excellent local control rates in both groups. Local failure occurred in only four of all patients—two each in the porta hepatis and non-porta hepatis groups. There were no significant differences in toxicities. Biliary stenosis associated with C-ion RT did not occur in either group. Therefore, in certain patients with a higher risk of injury to the bile duct when undergoing RFA, in high-risk cases such as elderly patients for postoperative complications after surgical resection, or in some patients who refuse to undergo hepatectomy or RFA, C-ion RT appears to offer a promising therapeutic alternative for HCC.

However, cause-specific and disease-free survival rates after 5 years were 25.0% [95% CI, 4–46] and 5.6% [95% CI, −5 to 16] in the porta hepatis group and 42.8% [95% CI, 27–58] and 23.9% [95% CI, 12–36] in the non-porta hepatis group, respectively, which indicates a difference which is of borderline significance ($P = 0.086$, $P = 0.051$). The presence of vascular invasion is higher in the porta hepatis group ($P = 0.066$). A characteristic of HCC is the potential of causing intrahepatic metastasis via vascular invasion, and therefore the cause-specific and disease-free survival rates are mainly representing the rate of intrahepatic metastases/new tumors as there were almost no local failures (Fig. 2). This emphasizes the necessity to take into account the possibility of intrahepatic metastasis via vascular invasion. Of course, the importance of the earliest possible detection of a new tumor lesion and its treatment with an appropriate therapeutic modality cannot be overstated. In this regard, it is considered especially important to keep in mind the clinical multidisciplinary approach available for treating HCC.

As for radiation therapy for HCC adjacent to the porta hepatis, it was reported that proton beam therapy delivering 72.6 GyE in 22 fractions appears effective and safe. Overall 3-year survival and local control rates were 45.1% and 86.0%, respectively [40]. In our study, these rates in the porta hepatis group were 44.4% [95% CI, 22–67] and 87.8% [95% CI, 72–104], respectively. Therefore, the treatment effect of short-course C-ion RT is suggested to be almost equal to that of proton beam therapy with a more fractionated regimen.

A limitation of this study was the fact that the patient number in the porta hepatis group was small. It is therefore important to collect such cases and continuously verify efficacy and safety of short-course C-ion RT for patients with HCC adjacent to the porta hepatis.

In conclusion, excellent local control was achieved independent of tumor localization. There was no significant difference in treatment-related toxicity between the porta hepatis and non-porta hepatis groups. The short-course C-ion RT of 52.8 GyE in four fractions appears to be an effective and safe therapeutic option for porta hepatis patients just as it is for non-porta hepatis patients.

Conflict of interest statement

Any actual or potential conflicts of interest do not exist.

Acknowledgements

This study was supported by the Research Project with Heavy Ions of the National Institute of Radiological Sciences in Japan. We are grateful to the members of the National Institute of Radiological Sciences.

References

[1] Bosch FX, Ribes J, Borras J. Epidemiology of primary liver cancer. Semin Liver Dis 1999;19:271–85.
[2] Phillips R, Murakami K. Preliminary neoplasms of the liver. Results of radiation therapy. Cancer 1960;13:714–20.
[3] Stillwagon GB, Order SE, Guse C, et al. 194 Hepatocellular cancers treated by radiation and chemotherapy combinations: Toxicity and response: a Radiation Therapy Oncology Group study. Int J Radiat Oncol Biol Phys 1989;17:1223–9.
[4] Robertson JM, Lawrence TS, Dworzanin LM, et al. Treatment of primary hepatobiliary cancers with conformal radiation therapy and regional chemotherapy. J Clin Oncol 1993;11:1286–93.
[5] Toya R, Murakami R, Baba Y, et al. Conformal radiation therapy for portal vein tumor thrombosis of hepatocellular carcinoma. Radiother Oncol 2007;84:266–71.

[6] Xi M, Liu MZ, Deng XW, et al. Defining internal target volume (ITV) for hepatocellular carcinoma using four-dimensional CT. Radiother Oncol 2007;84:272–8.
[7] Zhao JD, Xu ZY, Zhu J, et al. Application of active breathing control in 3-dimensional conformal radiation therapy for hepatocellular carcinoma: the feasibility and benefit. Radiother Oncol 2008;87:439–44.
[8] Suit HD, Goitein M, Munzenrider J, et al. Increased efficacy of radiation therapy by use of proton beam. Strahlenther Onkol 1990;166:40–4.
[9] Matsuzaki Y, Osuga T, Saito Y, et al. A new, effective, and safe therapeutic option using proton irradiation for hepatocellular carcinoma. Gastroenterology 1994;106:1032–41.
[10] Matsuzaki Y. The efficacy of powerful proton radiotherapy for hepatocellular carcinoma-long term effects and QOL. Ann Cancer Res Ther 1998;7:9–17.
[11] Blakely EA, Ngo FQH, Curtis SB, et al. Heavy ion radiobiology: cellular studies. Adv Radiat Biol 1984;11:295–378.
[12] Castro JR. Future research strategy for heavy ion radiotherapy. In: Kogelnih HD, editor. Progress in radio-oncology. Bologna: Monduzzi Editore; 1995. p. 643–8.
[13] Sato K, Yamada H, Ogawa K, et al. Performance of HIMAC. Nucl Phys 1995;A588:229–34.
[14] Kanai T, Furusawa Y, Fukutsu K, Itsukaichi H, Eguchi-Kasai K, Ohara H. Irradiation of mixed beam and design of spread-out Bragg peak for heavy-ion radiotherapy. Radiat Res 1997;147:78–85.
[15] Kanai T, Endo M, Minohara S, et al. Biophysical characteristics of HIMAC clinical irradiation system for heavy-ion radiation therapy. Int J Radiat Oncol Biol Phys 1999;44:201–10.
[16] Tsujii H, Morita S, Miyamoto T, et al. Preliminary results of phase I/II carbon ion therapy. J Brachyther Int 1997;13:1–8.
[17] Kato H, Tsujii H, Miyamoto T, et al. Results of the first prospective study of carbon ion radiotherapy for hepatocellular carcinoma with liver cirrhosis. Int J Radiat Oncol Biol Phys 2004;59:1468–76.
[18] Tsujii H, Mizoe JE, Kamada T, et al. Overview of clinical experiences on carbon ion radiotherapy at NIRS. Radiother Oncol 2004;73:S41–49.
[19] Kato H, Yamada S, Yasuda S, et al. Phase II study of short-course carbon ion radiotherapy (52.8 GyE/4-fraction/1-week) for hepatocellular carcinoma. Hepatology 2005;42:381A.
[20] Ikai I, Arii S, Okazaki M, et al. Report of the 17th nationwide follow-up survey of primary liver cancer in Japan. Hepatol Res 2007;37:676–91.
[21] Mulcahy MF. Management of hepatocellular cancer. Curr Treat Options Oncol 2005;6:423–35.
[22] Mazzaferro V, Regalia E, Doci R, et al. Liver transplantation for the treatment of small hepatocellular carcinomas in patients with cirrhosis. N Engl J Med 1996;334:693–9.
[23] Llovet JM, Fuster J, Bruix J. Intention-to-treat analysis of surgical treatment for early hepatocellular carcinoma: resection versus transplantation. Hepatology 1999;30:1434–40.
[24] Yoo HY, Patt CH, Geschwind JF, et al. The outcome of liver transplantation in patients with hepatocellular carcinoma in the United States between 1988 and 2001: 5-year survival has improved significantly with time. J Clin Oncol 2003;21:4329–35.
[25] Kuvshinoff BW, Ota DM. Radiofrequency ablation of liver tumors: influence of technique and tumor size. Surgery 2002;132:605–11.
[26] Shiina S, Teratani T, Obi S, et al. A randomized controlled trial of radiofrequency ablation with ethanol injection for small hepatocellular carcinoma. Gastroenterology 2005;129:122–30.
[27] Sato M, Watanabe Y, Ueda S, et al. Microwave coagulation therapy for hepatocellular carcinoma. Gastroenterology 1996;110:1507–14.
[28] Patterson EJ, Scudamore CH, Owen DA, et al. Radiofrequency ablation of porcine liver in vivo: effects of blood flow and treatment time on lesion size. Ann Surg 1998;227:559–65.
[29] Livraghi T, Solbiati L, Meloni MF, et al. Treatment of focal liver tumors with percutaneous radio-frequency ablation: complications encountered in a multicenter study. Radiology 2003;226:441–51.
[30] Nakazawa T, Kokubu S, Shibuya A, et al. Radiofrequency ablation of hepatocellular carcinoma: correlation between local tumor progression after ablation and ablative margin. AJR Am J Roentgenol 2007;188:480–8.
[31] Ohnishi T, Yasuda I, Nishigaki Y, et al. Intraductal chilled saline perfusion to prevent bile duct injury during percutaneous radiofrequency ablation for hepatocellular carcinoma. J Gastroenterol Hepatol 2008;23:e410–415.
[32] Llovet JM, Bru C, Bruix J. Prognosis of hepatocellular carcinoma: the BCLC staging classification. Semin liver Dis 1999;19:329–38.
[33] Llovet JM, Burroughs A, Bruix J. Hepatocellular carcinoma. Lancet 2003;362:1907–17.
[34] Minohara S, Kanai T, Endo M, Noda K, Kanazawa M. Respiratory gated irradiation system for heavy-ion radiotherapy. Int J Radiat Oncol Biol Phys 2000;47:1097–103.
[35] Suzuki M, Kase Y, Yamaguchi H, Kanai T, Ando K. Relative biological effectiveness for cell-killing effect on various human cell lines irradiated with heavy-ion medical accelerator in Chiba (HIMAC) carbon-ion beams. Int J Radiat Oncol Biol Phys 2000;48:241–50.
[36] Hasegawa K, Kokudo N, Imamura H, et al. Prognostic impact of anatomic resection for hepatocellular carcinoma. Ann Surg 2005;242:252–9.
[37] Rossi S, Garbagnati F, Lencioni R, et al. Percutaneous radio-frequency thermal ablation of nonresectable hepatocellular carcinoma after occlusion of tumor blood supply. Radiology 2000;217:119–26.
[38] McGhana JP, Dodd 3rd GD. Radiofrequency ablation of the liver: current status. AJR Am J Roentgenol 2001;176:3–16.
[39] de Baere T, Denys A, Wood BJ, et al. Radiofrequency liver ablation: experimental comparative study of water-cooled versus expandable systems. AJR Am J Roentgenol 2001;176:187–92.
[40] Mizumoto M, Tokuuye K, Sugahara S, et al. Proton beam therapy for hepatocellular carcinoma adjacent to the prota hepatis. Int J Radiat Oncol Biol Phys 2008;71:462–7.

British Journal of Cancer (2010) 103, 223–231

www.bjcancer.com

Increased circulating cell signalling phosphoproteins in sera are useful for the detection of pancreatic cancer

S Takano*[,1], K Sogawa[2,3], H Yoshitomi[1], T Shida[1], K Mogushi[4], F Kimura[1], H Shimizu[1], H Yoshidome[1], M Ohtsuka[1], A Kato[1], T Ishihara[5], H Tanaka[4], O Yokosuka[5], F Nomura[2,3] and M Miyazaki[1]

[1]Department of General Surgery, Graduate School of Medicine, Chiba University, 1-8-1 Inohana, Chuo-ku, Chiba 260-8670, Japan; [2]Department of Molecular Diagnosis, Graduate School of Medicine, Chiba University, Chiba, Japan; [3]Clinical Proteomics Research Center, Chiba University Hospital, Chiba, Japan; [4]Information Center for Medical Sciences, Tokyo Dental and Medical University, Tokyo, Japan; [5]Department of Medicine and Clinical Oncology, Graduate School of Medicine, Chiba University, Chiba, Japan

BACKGROUND: Intracellular phosphoprotein activation significantly regulates cancer progression. However, the significance of circulating phosphoproteins in the blood remains unknown. We investigated the serum phosphoprotein profile involved in pancreatic cancer (PaCa) by a novel approach that comprehensively measured serum phosphoproteins levels, and clinically applied this method to the detection of PaCa.

METHODS: We analysed the serum phosphoproteins that comprised cancer cellular signal pathways by comparing sera from PaCa patients and benign controls including healthy volunteers (HVs) and pancreatitis patients.

RESULTS: Hierarchical clustering analysis between PaCa patients and HVs revealed differential pathway-specific profiles. In particular, the components of the extracellular signal-regulated kinase (ERK) signalling pathway were significantly increased in the sera of PaCa patients compared with HVs. The positive rate of p-ERK1/2 (82%) was found to be superior to that of CA19-9 (53%) for early stage PaCa. For the combination of these serum levels, the area under the receiver-operator characteristics curves was showing significant ability to distinguish between the two populations in independent validation set, and between cancer and non-cancer populations in another validation set.

CONCLUSION: The comprehensive measurement of serum cell signal phosphoproteins is useful for the detection of PaCa. Further investigations will lead to the implementation of tailor-made molecular-targeted therapeutics.

British Journal of Cancer (2010) **103,** 223–231. doi:10.1038/sj.bjc.6605734 www.bjcancer.com
Published online 15 June 2010

Keywords: serum marker; pancreatic cancer; phospho-extracellular signal-regulated kinase; early diagnosis; cell signalling

Pancreatic cancer (PaCa) is an exceptionally devastating disease with a 5-year survival rate of only 5% (Jemal *et al*, 2009). One of the most crucial reasons for the poor prognosis is the lack of early diagnostic markers for PaCa. To overcome pancreatic malignancy, there is an urgent need to discover highly sensitive markers for early detection. The widely used serum-circulating marker for PaCa, carbohydrate tumour-associated antigen 19-9 (CA19-9), is not sufficiently accurate to be used as a diagnostic marker. CA19-9 is elevated in only approximately 65% of individuals with a resectable PaCa, and is also frequently elevated in patients with various benign pancreaticobiliary disorders; notably cholestasis and chronic pancreatitis (PT) (Goggins, 2005). Thus, CA19-9 is not recommended for diagnostic purposes (Locker *et al*, 2006).

In the past decade, various approaches have been used to discover new cancer serum biomarkers, and have identified some attractive molecular targets as diagnostic or prognostic markers for PaCa (Gold *et al*, 2006; Takano *et al*, 2008). Despite the identification of candidate proteins that have high diagnostic sensitivity and specificity in validation tests, translating these research findings to useful and reliable clinical tests still remains difficult (Zhang *et al*, 2004; Petricoin *et al*, 2002).

Protein phosphorylation is one of the most prominent, and intensively studied post-translational modifications in biological systems. Specifically, better understanding of the defective or hyperactive signalling pathways in cancer cells has been the major focus of mechanistic studies of cancer progression and differentiation, as well as in the identification of candidate markers for diagnosis and therapeutic targets (Petricoin *et al*, 2005). Ultimately, the signalling pathways promote tumourigenesis through the coordinated phosphorylation of proteins that directly regulate protein synthesis, cell-cycle progression and of transcription factors that regulate the expression of genes involved in these processes. Although these intracellular signalling pathways and its components (activated or inactivated forms) that are closely associated with cancer progression are among the most thoroughly studied in molecular cancer research, there has been little understanding of the dynamic nature of these circulating proteins in the bloodstream.

Because blood continuously perfuse the tissues of the body, it is thought to contain most human proteins (at least in fragment

*Correspondence: Dr S Takano; E-mail: stakano@faculty.chiba-u.jp
Received 23 February 2010; revised 10 May 2010; accepted 16 May 2010; published online 15 June 2010

forms), thereby supplying the richest and most detailed source of information about the physiological state of the body (Anderson *et al*, 2004). Thus, blood has a pivotal role in early disease detection. The turnover of proteins in cells requires calculated degradation processes to secrete intact or fragment forms into blood and to also remove proteins that are no longer necessary or those that have lost functional capabilities. Meanwhile, it is thought that a large part of those human serum-circulating proteins that promote signal transduction in cells may be cleaved by degradation of endogenous substrates and proteases (Villanueva *et al*, 2006a, b; Schilling and Knapp, 2008). Taken together, it is worthwhile for the early cancer detection to elucidate the molecular networks in cancerous cells and the microenvironments, and to investigate the dynamic nature of those cancer-related phosphorylated proteins including the fragments in circulating blood.

The Bio-Plex suspension array using specific antibodies and based on the principle of flow cytometry is a high-throughput technology that can measure multiple proteins in low sample volumes. Immunoaffinity approaches, particularly phospho-specific antibodies that recognise low abundance phospho-tyrosine, -serine and -threonine residues in the specific epitopes, have been used to assess phosphoprotein enrichment. In further developing this technology, it is possible to detect the phospho-specific sites of the parent molecule and its degraded fragments in serum as early diagnostic markers by comprehensive analysis in cancer patients. This technology has overcome a critical problem for the translational application of proteomics by developing a procedure that is convenient with high sensitivity, specificity and reproducibility. Moreover, this may also provide important information regarding the activation state of kinase-driven signalling networks in each cancer patient for therapeutic target selection with the advantage that the screen is less invasive.

In this study, we analysed the circulating cell signalling phosphoproteins in sera using this proteomic approach and investigated whether these protein levels are useful for detection, as early diagnostic serum markers for PaCa, in combination with comprehensive and hierarchical cluster analyses. Our study results indicate that the use of this new approach will lead to new insights in proteomic cancer biology and in the potential development of patient-tailored combination molecular targeting therapy, through elucidation of the phosphoprotein networks in serum from cancer patients.

MATERIALS AND METHODS

Patient samples

We selected four populations of patients with PaCa, PT and healthy control volunteer (HV). Blood samples were obtained from all patients who were diagnosed with PaCa and PT in the Chiba University Hospital, Chiba, Japan, from November 2002 to March 2009, and the samples were also obtained from HVs in the Chiba University Hospital and the Kashiwado Hospital, Chiba, Japan. Sera were collected from 26 patients with PaCa and 25 HVs for the training set, from 80 patients with PaCa and 68 HVs for validation set 1, furthermore, to assess the diagnostic ability of discriminating between cancer and non-cancer populations, sera of 35 patients with PaCa as a cancer group, and 40 patients with PT as well as 48 HVs as a non-cancer group were selected to match for age for validation set 2 (Table 1). All patients were histologically confirmed as PaCa. The characteristics of 141 patients with PaCa are summarised in Table 2. All blood samples were processed according to a standardised protocol, and serum sample aliquots were frozen until the subsequent analysis. None of the patients received any therapeutic treatments, such as radiation, chemotherapy or operation, until serum samples were collected.

Table 1 Summary of all participants

Experimental groups (number of patients)	Sex (M/F)	Age (mean ± s.d.)
Training set (n = 51)		
Pancreatic cancer (n = 26)	17/9	65.2 ± 8.0
Healthy volunteer (n = 25)	17/8	52.0 ± 10.6
Validation set 1 (n = 148)		
Pancreatic cancer (n = 80)	48/32	62.9 ± 10.8
Healthy volunteer (n = 68)	41/27	54.1 ± 6.8
Validation set 2 (n = 123)		
Pancreatic cancer (n = 35)	21/14	63.6 ± 8.8
Pancreatitis (n = 40)	38/2	61.7 ± 8.8
Healthy volunteer (n = 48)	32/16	62.4 ± 7.3

Abbreviations: F = female; M = male.

Table 2 Characteristics of patients with pancreatic cancer

Variables	Training set (n = 26)	Validation set 1 (n = 80)	Validation set 2 (n = 35)
Tumor stage			
T1	0	3	8
T2	2	2	4
T3	21	47	12
T4	2	10	2
TX	1	18	9
Nodal status			
N0	7	16	16
N1	17	41	10
NX	2	23	9
Metastasis			
M0	24	53	30
M1	2	27	5
UICC stage			
IA	0	2	8
IB	1	2	4
IIA	6	11	3
IIB	16	32	10
III	1	6	5
IV	2	27	5
Resection status			
R0	12	38	21
R1	7	9	5
R2	4	6	0
RX	3	27	9

Abbreviations: RX = unresectable case; UICC = Union Internationale Contre le Cancer.

The ethics committee for each institute approved the protocol. Written informed consent was obtained from all patients and HVs.

Bio-Plex phosphoprotein suspension assay

Phosphorylated proteins in serum were detected with a Bio-Rad phosphoprotein immunoassay kit using the Bio-Plex 200 suspension array system (Bio-Rad Laboratories, Hercules, CA, USA). The human serum diluent buffer was added up to 50 μl to the eight-fold diluted samples, 50 μl aliquots of each of the diluted samples were plated in the 96-well filter plate, coated with anti-phosphoprotein antibody-coupled beads, and incubated for 16 h on a platform shaker at 300 r.p.m. at room temperature. The wells were vacuum

filtered and washed, 1 μl of detection antibodies (25 ×) was added, vortexed and incubated for 30 min. After additional vacuum filtration and washing of the wells, 0.5 μl streptavidin-PE (100 ×) was added to each well and allowed to incubate for 10 min. The wells were again vacuum filtered and washed, 125 μl of re-suspension buffer was added and incubated for 30 s. Data acquisition and analysis were performed using Bio-Plex Manager software version 5.0. The data of measurement by the Bio-Plex 200 suspension array system are presented in the Supplementary Information (Supplementary Figure S1; Supplementary Table S1).

For the training set, 18 targeted phosphorylated (p-) proteins were measured using Bio-Plex 200 suspension array system in the comprehensive phosphoprotein analysis. Focusing on the more promising candidate proteins, phospho-mitogen-regulated kinase 1 (p-MEK1), phospho-extracellular signal-regulated kinases 1/2 (p-ERK1/2) and those total proteins; we measured (*t*-) for the further validation sets.

Immunohistochemistry

Paraffin-embedded tissues were cut into 4 μm-thick serial sections and were de-paraffinised. Serial section slides were placed in citric acid buffer (10 mmol l^{-1}, pH 6.0) with 0.2% Tween 20 and boiled in a microwave oven (2 × 6 min) to retrieve the antigen. The slides were then rinsed and blocked in a 3% H_2O_2 solution with methanol for 10 min, before being incubated overnight at 4°C with the primary antibodies; rabbit anti-phospho-MEK1/2 monoclonal antibody (Cell Signaling Technology, Beverly, MA, USA) and rabbit anti-phospho-ERK1/2 (p44/42 MAPK) monoclonal antibody (Cell Signaling Technology) (1 : 50 and 1 : 200 dilution respectively). SignalStain Antibody Diluent (Cell Signaling Technology) was used as the dilution buffer. They were then rinsed in PBS, and incubated for 60 min with secondary antibody labelled with streptoavidin-biotin-peroxidase (DAKO LSAB+ kit; DakoCytomation, Glostrup, Denmark). The bound complex was visualised using diaminobenzidine liquid chromogen and counterstained with hematoxylin.

Comprehensive and hierarchical clustering analyses of the training and validation sets

To investigate the similarity of expression patterns, we performed hierarchical clustering analysis using R statistical software (version 2.8.0). Before analysis, the expression levels were standardised using *Z*-transformation (mean = 0 and variance = 1) for each protein. We then used Euclidian distance of expression patterns for calculation of distance matrices (i.e., one for proteins and the other for samples) between each variable, as well as the average linkage method for clustering analysis.

Multivariate logistic regression using selected proteins

To assess the diagnostic ability for PaCa patients and controls, we performed univariate and multivariate logistic regression analyses using p-ERK1/2, CA19-9 and the combination of p-ERK1/2 and CA19-9 models. Receiver-operating characteristic (ROC) curves and area under the curve (AUC) based on the prediction results of the obtained regression models were calculated by the R statistical software.

Statistical analysis

Statistical analyses were performed using the appropriate tests as indicated. *P*-values <0.05 were considered statistically significant. To compare the positive rate for detecting early stage pancreatic malignancies, we determined the positive levels of p-ERK1/2 in disease patients by the reference values in each of the respective three sets (Solberg, 1987). The reference values in the three sets were calculated using reference limits corresponding to 0.95 fraction of the distribution, that is the upper limit of the 95% confidence interval (CI), in the three respective healthy control groups. For CA19-9, a cut-off value of 37 IU ml^{-1} was used, according to the manufacturer's specifications for the reference range of CA19-9.

RESULTS

Circulating phosphoproteins levels are increased in sera from patients with pancreatic cancer

To detect new biomarkers characteristic of the PaCa patients, we comprehensively first measured the 18 major targeted cell signalling phosphoproteins levels in sera of the training set using the Bio-Plex suspension array. Many of the target phosphoproteins levels were increased significantly in sera from PaCa patients compared with the HVs (see detail of the experimental data in Supplementary Table S2). Hierarchical clustering analysis showed that the relative differential expressions of circulating phosphoproteins clearly distinguished PaCa patients from HVs (Figure 1A). Six candidate phosphoproteins (p-ERK1/2: $P<0.00001$, p-MEK1: $P<0.0005$, phospho-p90 ribosomal S6 kinase (p-p90RSK): $P<0.0001$, phospho-cAMP response element binding protein (p-CREB): $P<0.00001$, p-Akt: $P<0.00005$ and p-IκB-α: $P<0.0001$; Mann-Whitney *U*-test) were significantly increased in sera from patients with PaCa compared with the HVs.

As shown in the lower panel of Figure 1A, similar cluster structures were obtained in the clustering analysis of these six phosphoproteins. Subclass analysis separated the PaCa patients into two groups, based on hierarchical clustering of the six candidate marker levels, and revealed that each of the two groups correlated well with the groups that had favourable and unfavourable prognoses ($P=0.07$; log-rank test; Figure 1B). These were also closely correlated with each protein belonging to the phosphatidylinositol-3-OH kinase/Akt, NF-κB and ERK signalling pathways that are crucial for cancer survival (Figure 1C).

Two of these proteins, p-ERK1/2 and p-MEK1, are shown in Figure 2A. Of particular interest, four of the six phosphoproteins were proteins directly associated with the most popular pathway of pancreatic carcinogenesis, the Ras/Raf/MEK/ERK signalling cascade to two proteins (p-p90RSK and p-CREB) that are directly or indirectly phosphorylated by ERK. Surprisingly, the results indicate that p-ERK1/2 levels in serum showed a significantly positive correlation with p-MEK1 levels ($r=0.57$, $P<0.00002$; Pearson's correlation coefficient test) as well as p-ERK, which would theoretically be dependant on the activity of MEK and is in turn promoted by an entire series of upstream events (Figure 2B). Therefore, we mainly selected two key molecules, ERK and MEK, to investigate the expression of those phosphorylated and total proteins in sera for further validation analyses by Bio-Plex assay.

Confirmation of target phosphoprotein serum levels by western blot analysis

To confirm the results obtained from Bio-Plex assay, we assessed the expression of phosphoproteins both sera from patients with PaCa and HVs by immunoprecipitation assay and western blot analysis. Corresponding with Bio-Plex data, increased p-ERK1/2 expression levels were confirmed by western blot analysis in sera from three PaCa patients and one HV (see detail of the methods and experimental data in Supplementary Figure S2).

Activated p-ERK and p-MEK are expressed in pancreatic cancer cells

To examine the potential source of the activated ERK and MEK in serum, we performed immunohistochemical staining for these phosphoproteins in resected PaCa tissues. As shown in Figure 2C,

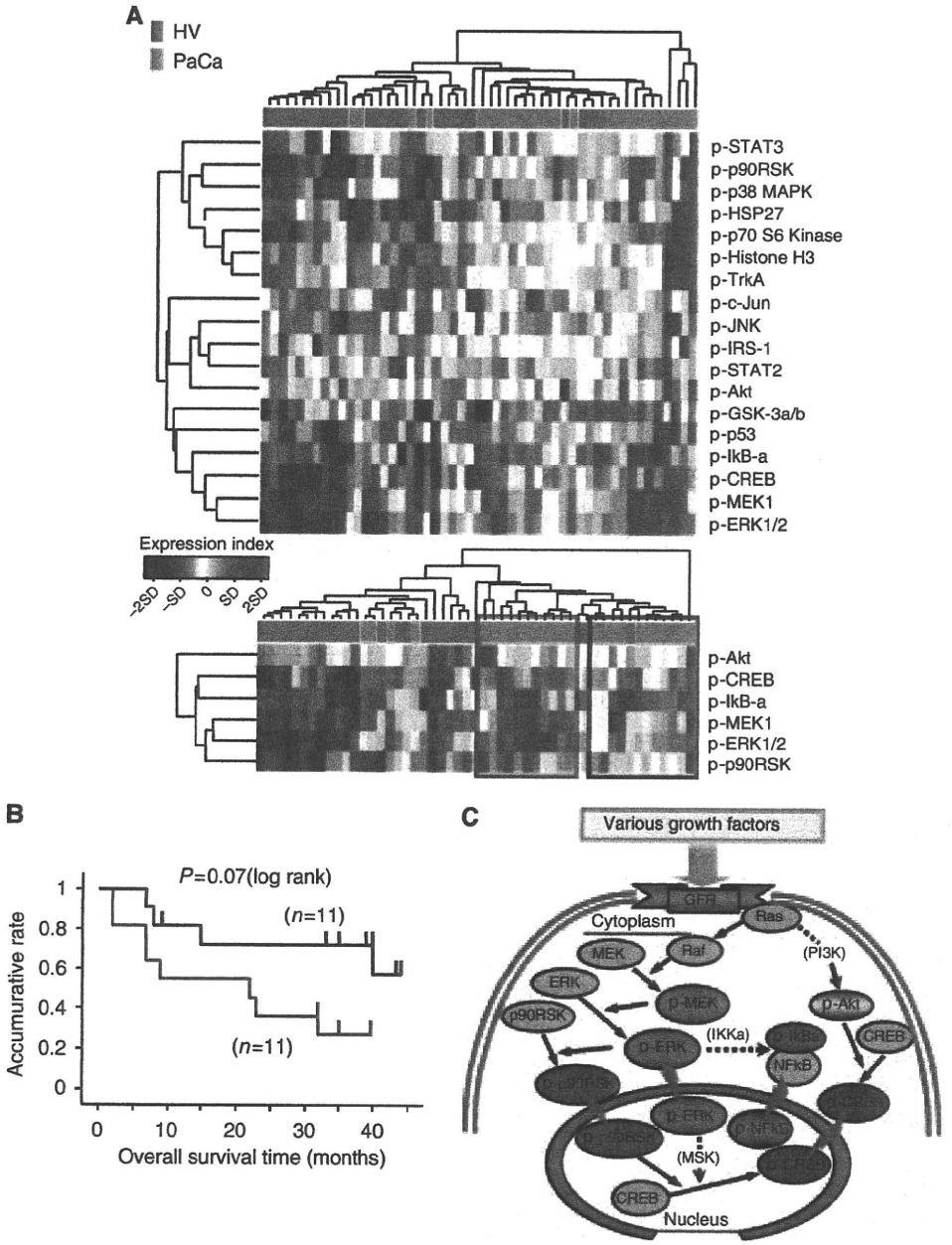

Figure 1 Hierarchical clustering of phosphoprotein expression profiles in the training set. (**A**) Healthy volunteers (HVs) are denoted in light blue in the vertical side bar, and pancreatic cancer (PaCa) patients are denoted in orange. Dendrograms show the classification determined by hierarchical clustering analysis of 18 targeted phosphoproteins. As shown in Expression index, red and blue in the matrix indicate relative overexpression and underexpression respectively (s.d.; standard deviation). The hierarchical clustering analysis clearly distinguished the two groups; the majority of PaCa patients are found in the right side, whereas HVs are mainly located in the left side of the heat map (upper panel). The profiles of six candidate circulating phosphoproteins associated with PaCa are revealed by hierarchical clustering analysis (lower panel). Subclass analysis separated the PaCa patients into two groups based on the candidate phosphoproteins. The distinction of the two groups is indicated by the blue and purple lined boxes. (**B**) Kaplan–Meier analysis revealed that each of the two groups (blue and purple lines) distinguished by the hierarchical clustering analysis was well matched with a favourable and unfavourable prognosis of PaCa patient groups. (**C**) The schema of the correlation between candidate phosphoproteins by cell signal transduction in the intracellular environment. The crucial interaction among these molecules allows the cancer to proliferate and differentiate through representative cell signalling pathways.

both activated p-ERK and p-MEK expression levels were clearly positive in pancreatic ductal carcinoma cells. The p-ERK and p-MEK expression was localised to the neoplastic epithelial cells and some stromal cells especially surrounding the ductal carcinoma cells. Activated p-ERK was found in both the nucleus and cytoplasm of cancer cells. Conversely, p-MEK expression was not found in the nucleus of cancer cells, but stained intensely in the cytoplasm of cancer cells.

Both p-ERK and p-MEK levels in sera were significantly correlated with the positive staining of pancreatic cancer tissues

Next, we investigated whether the two phosphoproteins levels in sera correlated with the positive staining in PaCa tissues. Among 26 PaCa patients in training set, 23 patients (R0, R1 and R2; all resectable cases) were analysed by immunohistochemical staining

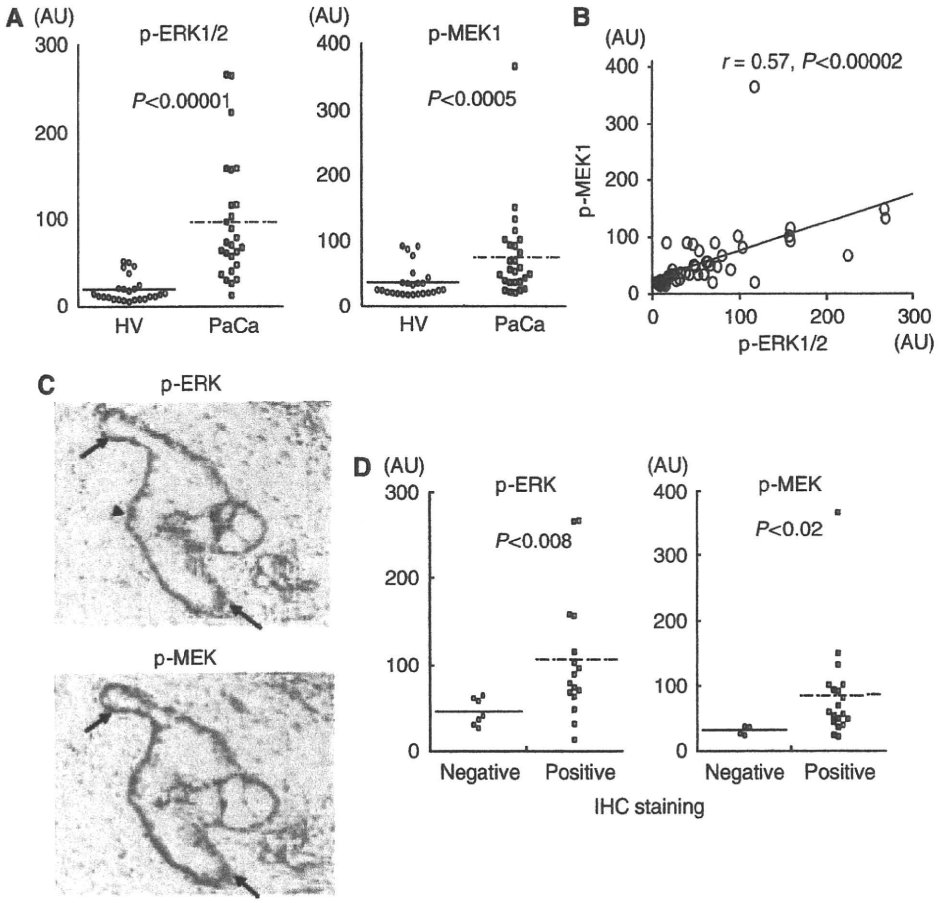

Figure 2 Serum phosphoproteins increased in PaCa patients compared to HVs in the training set. (**A**) Circulating p-ERK1/2 and p-MEK1 levels in sera are significantly greater in PaCa patients than HVs. (**B**) Linear regression with p-ERK1/2 and p-MEK1 levels reveals a significant, positive correlation in the training set. (**C**) Immunostaining for p-ERK and p-MEK in PaCa tissues (original magnification, × 200). Note that expression of the two phosphoproteins is evident in the cancerous cytoplasm (arrows in p-ERK and p-MEK) and nucleus (arrowhead in p-ERK), and is also found in stromal cells surrounding the ductal carcinoma cells. (**D**) Both p-ERK and p-MEK levels in sera were significantly correlated with the positive staining of PaCa tissues (p-ERK: $P<0.008$, p-MEK: $P<0.02$; Mann–Whitney *U*-test).

of the PaCa tissues. The 23 patients were divided into two groups based on positive or negative staining in PaCa cells, 16 (69.6%) of 23 cases were p-ERK-positive staining, and 19 (82.6%) cases were p-MEK-positive staining. Notably, as shown in Figure 2D, both p-ERK and p-MEK levels in sera were significantly correlated with the positive staining of PaCa tissues respectively (p-ERK: $P<0.008$, p-MEK: $P<0.02$; Mann–Whitney *U*-test).

Both phospho- and total-ERK1/2 simultaneously increase with a positive correlation in sera of patients with pancreatic cancer

To confirm the results obtained from the training set, we measured and analysed both ERK and MEK serum levels with an increased sample size in validation set 1. Similar results were obtained, that both p-ERK1/2 and p-MEK1 levels were significantly increased in sera from PaCa patients compared with that of HVs for validation set 1 (p-ERK1/2; $P<0.00001$, p-MEK1; $P<0.00001$: Mann–Whitney *U*-test; Figure 3A). In addition, t-ERK1/2 levels were also significantly more upregulated in sera from PaCa patients compared with that of HVs in validation set 1 ($P<0.00001$; Mann–Whitney *U*-test). Of particular interest, both p- and t-ERK1/2 levels increased simultaneously with a positive correlation in sera from PaCa patients ($r=0.38$, $P<0.0004$; Pearson's correlation coefficient test) (figure not shown).

Phospho-ERK1/2 level in serum excels in the detection of pancreatic cancer

To estimate the cell signalling phosphoprotein, p-ERK1/2, as a novel serum biomarker to detect PaCa patients, we calculated the ROC curves, which correlate the true- and false-positive rates (sensitivity and 1 specificity) between PaCa patients and HVs. The area under the ROC curve (AUC) was 0.94 for p-ERK1/2, and concerning with other phosphoproteins, the AUCs were 0.79 for p-MEK1, 0.81 for p-p90RSK, 0.86 for p-CREB and 0.83 for p-Akt in the training set. To validate and compare the abilities of serum markers for the diagnosis of PaCa, we constructed ROC curves for p-ERK1/2, CA19-9 and the combination of two serum levels in validation set 1. The respective AUC was 0.88 for p-ERK1/2, 0.91 for CA19-9 and 0.96 for the combination p-ERK1/2 and CA19-9 (Figure 3B).

The positive rate of serum p-ERK1/2 in the disease groups was calculated using the reference values determined according to the upper limit of 95% CI in the three respective healthy control groups. In all three sets of this study, only five patients showed negative levels for both p-ERK1/2 and CA19-9. For CA19-9,

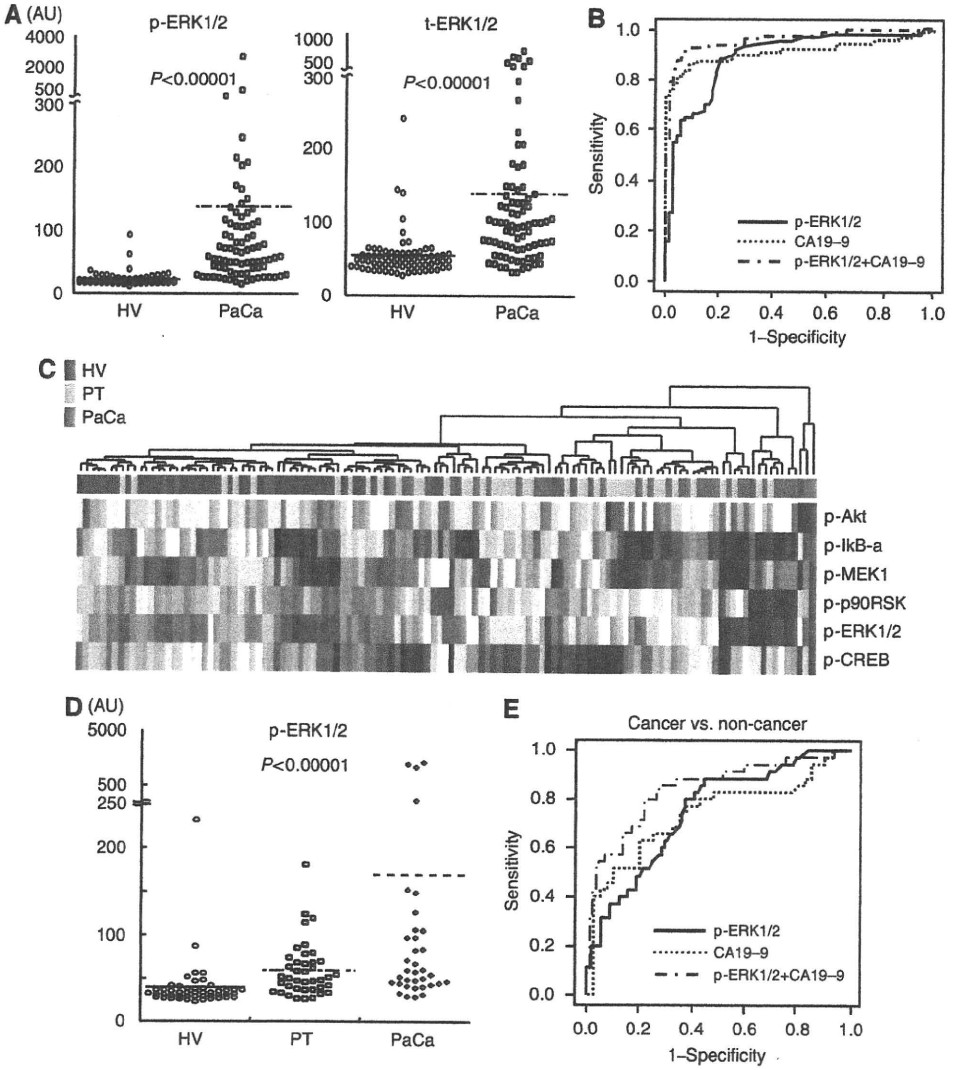

Figure 3 Confirmation of the results obtained from the training set for validation set 1. (**A**) The similar result of the training set shows that both circulating p-ERK1/2 and t-ERK1/2 levels were significantly increased in sera from PaCa patients compared with that of HVs for validation set 1. (**B**) The ROC analyses were performed for the serum levels of p-ERK1/2, CA19-9 and a combination of p-ERK1/2 and CA19-9 between PaCa patients and HVs. The respective AUCs were 0.88 for p-ERK1/2 level, 0.91 for CA19-9 level and 0.96 for the combination of p-ERK1/2 and CA19-9 levels. Comparing among three populations in validation set 2. (**C**) Serum levels of six candidate phosphoproteins were able to distinguish among the three populations (HV, PT and PaCa) by hierarchical clustering analysis. The analysis distinguished the three groups; the majority of PaCa patients are found on the right side, whereas PT are located diffusely in the approximate centre and HVs are mainly located on the left side of the heat map. (**D**) Circulating p-ERK1/2 levels in sera were significantly differenced among three populations (PaCa, PT and HVs) ($P<0.00001$; Kruskal–Wallis test). (**E**) The ROC analyses were performed for the serum levels of p-ERK1/2 and CA19-9 between cancer (PaCa) and non-cancer (HVs and PT) populations. The respective AUCs were 0.75 for p-ERK1/2 level and 0.70 for CA19-9 level and 0.84 for the combination of p-ERK1/2 and CA19-9 levels.

39 false-negative patients were mostly picked up as p-ERK1/2-positive (87.2%) patients with PaCa (Table 3). These results indicate that the combination of p-ERK1/2 and CA19-9 achieved sufficiently high sensitivity and specificity to diagnose PaCa accurately by supplementing the low sensitivity of CA19-9 that was caused by deficiency of Lewis antigens and so on.

Combination of p-ERK1/2 and CA19-9 levels is superior discriminatory power between cancer and non-cancer populations

In validation set 2, we compared and analysed the differential protein expression of six candidate phosphoproteins levels in sera from PaCa, PT patients and HVs. Hierarchical clustering analysis indicated that the populations of PT patients were located diffusely but approximately in between the HVs and PaCa patient groups (Figure 3C).

Furthermore, to assess the discriminatory power of serum p-ERK1/2 levels, we measured to compare p-ERK1/2 and CA19-9 levels in sera of PaCa patients and age-matched benign controls including PT patients. Phospho-ERK1/2 levels were significantly increased in sera among three populations ($P<0.00001$; Kruskal–Wallis test; Figure 3D), and between cancer and non-cancer populations ($P<0.00002$; Mann–Whitney U-test). To discriminate cancer from non-cancer groups, we performed multivariate logistic regression analysis using p-ERK1/2 and CA19-9. As a result, both p-ERK1/2 (odds ratio: 13.4, 95% CI: 2.14–83.6, $P=0.0056$; Wald test) and CA19-9 (odds ratio: 3.67, 95% CI: 1.86–7.22, $P=0.0002$;

Table 3 p-ERK1/2-positive rate in CA19-9 false-negative patients with pancreatic cancer

	CA19-9 false negative (%)	p-ERK1/2-positive in CA19-9 false negative (%)
Training set	6/26 (23.1)	6/6 (100.0)
Validation set 1	22/80 (27.5)	20/22 (90.9)
Validation set 2	11/35 (31.4)	8/11 (72.7)
Total	39/141 (27.7)	34/39 (87.2)

Abbreviations: CA19-9 = carbohydrate tumour-associated antigen 19-9; p-ERK1/2 = phospho-extracellular signal-regulated kinases 1/2.

Wald test) were identified as significant variables for the detection of PaCa. For distinguishing between cancer and non-cancer groups, the respective AUC was 0.75 for p-ERK1/2 and 0.70 for CA19-9, and the AUC was 0.84, showing high ability to distinguish between cancer and non-cancer groups, for the combination of the two serum levels (Figure 3E). These results suggest the combination of p-ERK1/2 and CA19-9 levels is better discriminatory power compare to CA19-9 alone between cancer and non-cancer populations.

Circulating p-ERK1/2 is a potential novel marker for early stage of pancreatic cancer

To emphasise the diagnosis of early stage of patients with pancreatic malignancy, we found that the sensitivity of serum p-ERK1/2 levels for predicting stage I PaCa in our study population was 82% (14 out of 17 patients with stage IA or IB cancers had elevated p-ERK1/2), whereas only 9 out of 17 (53%) patients showed elevated CA19-9. These results suggest that the measurement of serum p-ERK1/2 levels could be particularly helpful in the detection of early stage PaCa.

DISCUSSION

The results reported herein show that the measurement of circulating signal transduction proteins in serum led to the detection of PaCa. To elucidate molecules related to PaCa progression, we used a new strategy based on the multiplexed cell signalling of phosphoproteins in serum by hierarchical clustering analysis. To detect pre-malignant tumour or early stage malignancies, it is necessary to be able to assess very low abundant substances that are likely produced by tumour itself (i.e., fragments of cellular components, endo- or exogenous protease and secretion derived from tumour) (Villanueva *et al*, 2006a, b), the microenvironment of the tumour–host interface (Iacobuzio-Donahue *et al*, 2002) and the host immune response to tumour (Koomen *et al*, 2005). Recently, it was reported that both lymphatic vessel compression with resultant functional abnormalities and elevated interstitial fluid pressure occur during the early stages of carcinogenesis (Hagendoorn *et al*, 2006). These insights have formed the theoretical foundation for the detection of early stages of cancer.

Biological fluids, such as serum, are a readily obtainable source of potential cancer biomarkers that are shed or secreted by cancer cells, and are produced as a consequence of humoral immunity (Lu *et al*, 2008). Serum immerses most tissues in the body and is therefore likely to contain cell-derived proteins that can provide dynamic information about various biological processes. In addition, it is thought that cellular or tissue protein might likely present as a full-length form or the cleavage fragments that freely enter circulation by diffusion or convection (Liotta and Petricoin, 2006).

Concerning proteins as indicators, it has been recognised that blood protein biomarkers are amplified in the circulatory system because they accumulate on the high concentration of resident proteins, such as albumin, and then acquire the longer half-life of albumin, thereby protecting the bound species from renal clearance (Lowenthal *et al*, 2005; Araujo *et al*, 2008). Lowenthal *et al* also indicated that among many individual sequences that were predicted from albumin-associated proteins in serum from patients with three stages of ovarian cancer, the predicted sequences were largely fragments derived from proteins with diverse biological functions, including crucial cellular signal transduction factors. Interestingly, the kinds of signal transduction factors were more numerous in sera from patients with early stage than in advanced stage of cancer among the identified proteins. In an recent study, the enrichment of serum phosphopeptides using the modified particles was successful to identify phosphorylated peptides that were related to cancer. The profiling of these degraded fragments has been found to be able to distinguishing between hepatocellular carcinoma patients and healthy individuals (Hu *et al*, 2009). Our current study results are consistent with these theories of protein amplification and actual identification in the circulatory system.

The activation of epidermal growth factor receptor (EGFR) and the various downstream targets, such as Ras, Raf, MEK and ERK, are deeply implicated in the pathogenesis of PaCa with malignant transformation and enhanced tumour aggressiveness. In addition, the signalling cascade is likely crucial for PaCa progression because K-Ras gene mutations have been found in many populations of human PaCa specimens. The efficacy of molecular targeting therapies for PaCa, such as an inhibitor of EGFR tyrosine kinase, small-molecule inhibitor of Raf kinase and that of the dual specificity kinase MEK1/2, have recently being evaluated in some clinical trials, however, the results have not been impressive (Rinehart *et al*, 2004; Siu *et al*, 2006; Moore *et al*, 2007). The major reason is considered that the dysregulation or hyperactivity in the network of intracellular and extracellular signalling pathways is so complicated with multiplicity that each individual may have a differential profile even among similar malignancies. It is reasonable to surmise that to obtain maximum efficacy of molecular-targeted therapies it is necessary to investigate which pathway is more highly activated for each cancer patient (Jimeno *et al*, 2008). In the near future, our new insights may resolve this problem with a minimally invasive approach.

This is the first study to show circulating cell signalling phosphoproteins in blood of PaCa patients. In our experiments, comprehensive and hierarchical clustering analyses of serum phosphoproteins between PaCa patients and HVs revealed pathway-specific profiles, in particular components of the ERK signalling pathway, and a new method to classify serum phosphoproteins possibly derived from tumour itself, based on intracellular signalling portraits. As mentioned above, overcoming the issue of specificity as well as discovering highly sensitive markers for early detection are undoubtedly important. We confirmed that this signature could be used to discriminate not only between cancer and healthy controls in an independent validation set but also between cancer and non-cancer populations in an age-matched sample as another validation set. We also found that these circulating molecules were potentially useful for the diagnosis of early stage PaCa. These results suggest that the level of circulating p-ERK may be associated with early stage of pancreas carcinogenesis.

Immunohistochemistry of PaCa tissues showed that two target phosphoproteins, p-ERK and p-MEK, were simultaneously well expressed during the early stage neoplasms, even in the cancer cells of non-invasive or minimally invasive ductal carcinoma, as well as in the advanced stage patients with PaCa. Furthermore,

both p-ERK and p-MEK levels in sera of PaCa patients were in good correlation with the positive staining of their PaCa tissues. Taken together, we consider that the major source for the elevation of cell signal phosphoproteins levels in serum may be cancer cells that are showing augmented cell signalling.

Subclasses distinguished by hierarchical clustering analysis of six candidate markers indicated good correlation with the prediction of the prognosis of PaCa patients in this study. Further investigation of subclass analysis by hierarchical clustering will provide fruitful information regarding which factors of cell signalling phosphoproteins in serum are associated with the malignant behaviour of PaCa.

PaCa develops as a result of the stimulation and activation of various growth factor receptors. The continuous stimulation of these signal transduction pathways leads to increases in both the activated and inactivated forms of the cell signalling molecules in the intracellular environments of cancerous cells. The downstream activation transmits information through post-translational protein modifications with reversible protein phosphorylation. Increasing signal molecules that accumulate in the cell trigger changes in the penetration of cell membrane, which causes the release of both phosphoproteins and the degraded fragments to extracellular environments by cellular apoptosis. Once released from the intracellular environments, those proteins likely lose their original function, and are then carried to nearby blood vessels, and circulate freely or with binding to high-affinity transfer proteins in blood circulatory system. However, further research is needed to elucidate the sequence of this pathway.

In conclusion, we found cancer-associated cell signal phosphoproteins in serum using multiplexed cell signalling analysis. The measurement of circulating phosphoproteins in serum was able to discriminate between cancer patients and benign controls, and this new approach was helpful in the early diagnosis of patients with PaCa. This method shows the feasibility of this analysis, with a less invasive approach. The next step is to elucidate the profiling of cell signal activation by these comprehensive and hierarchical clustering analyses may discriminate subclasses into clinically significant groups. In the near future, investigations determining the footprints of circulating phosphoproteins will lead to the clinical application of this method that will be used for targeted tailor-made therapeutics.

ACKNOWLEDGEMENTS

We thank Dr Takeshi Tomonaga and Dr Yoshio Kodera for helpful discussions, and Fumie Iida for technical support.

Supplementary Information accompanies the paper on British Journal of Cancer website (http://www.nature.com/bjc)

REFERENCES

Anderson NL, Polanski M, Pieper R, Gatlin T, Tirumalai RS, Conrads TP, Veenstra TD, Adkins JN, Pounds JG, Fagan R, Lobley A (2004) The human plasma proteome: a nonredundant list developed by combination of four resources. *Mol Cell Proteomics* **3:** 311–326

Araujo RP, Petricoin EF, Liotta LA (2008) Critical dependence of blood-borne biomarker concentrations on the half-lives of their carrier proteins. *J Theor Biol* **253:** 616–622

Goggins M (2005) Molecular markers of early pancreatic cancer. *J Clin Oncol* **23:** 4524–4531

Gold DV, Modrak DE, Ying Z, Cardillo TM, Sharkey RM, Goldenberg DM (2006) New MUC1 serum immunoassay differentiates pancreatic cancer from pancreatitis. *J Clin Oncol* **24:** 252–258

Hagendoorn J, Tong R, Fukumura D, Lin Q, Lobo J, Padera TP, Xu L, Kucherlapati R, Jain RK (2006) Onset of abnormal blood and lymphatic vessel function and interstitial hypertension in early stages of carcinogenesis. *Cancer Res* **66:** 3360–3364

Hu L, Zhou H, Li Y, Sun S, Guo L, Ye M, Tian X, Gu J, Yang S, Zou H (2009) Profiling of endogenous serum phosphorylated peptides by titanium (IV) immobilized mesoporous silica particles enrichment and MALDI-TOF MS detection. *Anal Chem* **81:** 94–101

Iacobuzio-Donahue CA, Ryu B, Hruban RH, Kern SE (2002) Exploring the host desmoplastic response to pancreatic carcinoma. *Am J Pathol* **160:** 91–99

Jemal A, Siegel R, Ward E, Hao Y, Xu J, Thun MJ (2009) Cancer statistics, 2009. *CA Cancer J Clin* **59:** 225–249

Jimeno A, Tan AC, Coffa J, Rajeshkumar NV, Kulesza P, Rubio-Viqueira B, Wheelhouse J, Diosdado B, Messersmith WA, Iacobuzio-Donahue C, Maitra A, Varella-Garcia M, Hirsch FR, Meijer GA, Hidalgo M (2008) Coordinated epidermal growth factor receptor pathway gene overexpression predicts epidermal growth factor receptor inhibitor sensitivity in pancreatic cancer. *Cancer Res* **68:** 2841–2849

Koomen JM, Shih LN, Coombes KR, Li D, Xiao LC, Fidler IJ, Abbruzzese JL, Kobayashi R (2005) Plasma protein profiling for diagnosis of pancreatic cancer reveals the presence of host response proteins. *Clin Cancer Res* **11:** 1110–1118

Liotta LA, Petricoin EF (2006) Serum peptidome for cancer detection: spinning biologic trash into diagnostic gold. *J Clin Invest* **116:** 26–30

Locker GY, Hamilton S, Harris J, Jessup JM, Kemeny N, Macdonald JS, Somerfield MR, Hayes DF, Bast Jr RC, ASCO (2006) ASCO 2006 update of recommendations for the use of tumor markers in gastrointestinal cancer. *J Clin Oncol* **24:** 5313–5327

Lowenthal MS, Mehta AI, Frogale K, Bandle RW, Araujo RP, Hood BL, Veenstra TD, Conrads TP, Goldsmith P, Fishman D, Petricoin III EF, Liotta LA (2005) Analysis of albumin-associated peptides and proteins from ovarian cancer patients. *Clin Chem* **51:** 1933–1945

Lu H, Goodell V, Disis ML (2008) Humoral immunity directed against tumor-associated antigens as potential biomarkers for the early diagnosis of cancer. *J Proteome Res* **7:** 1388–1394

Moore MJ, Goldstein D, Hamm J, Figer A, Hecht JR, Gallinger S, Au HJ, Murawa P, Walde D, Wolff RA, Campos D, Lim R, Ding K, Clark G, Voskoglou-Nomikos T, Ptasynski M, Parulekar W, National Cancer Institute of Canada Clinical Trials Group (2007) Erlotinib plus gemcitabine compared with gemcitabine alone in patients with advanced pancreatic cancer: a phase III trial of the National Cancer Institute of Canada Clinical Trials Group. *J Clin Oncol* **25:** 1942–1952

Petricoin EF, Ardekani AM, Hitt BA, Levine PJ, Fusaro VA, Steinberg SM, Mills GB, Simone C, Fishman DA, Kohn EC, Liotta LA (2002) Use of proteomic patterns in serum to identify ovarian cancer. *Lancet* **359:** 572–577

Petricoin EF, Bichsel VE, Calvert VS, Espina V, Winters M, Young L, Belluco C, Trock BJ, Lippman M, Fishman DA, Sgroi DC, Munson PJ, Esserman LJ, Liotta LA (2005) Mapping molecular networks using proteomics: a vision for patient-tailored combination therapy. *J Clin Oncol* **23:** 3614–3621

Rinehart J, Adjei AA, Lorusso PM, Waterhouse D, Hecht JR, Natale RB, Hamid O, Varterasian M, Asbury P, Kaldjian EP, Gulyas S, Mitchell DY, Herrera R, Sebolt-Leopold JS, Meyer MB (2004) Multicenter phase II study of the oral MEK inhibitor, CI-1040, in patients with advanced non-small cell lung, breast, colon, and pancreatic cancer. *J Clin Oncol* **22:** 4456–4462

Schilling M, Knapp DR (2008) Enrichment of phosphopeptides using biphasic immobilized metal affinity-reversed phase microculumns. *J Proteome Res* **7:** 4164–4172

Siu LL, Awada A, Takimoto CH, Piccart M, Schwartz B, Giannaris T, Lathia C, Petrenciuc O, Moore MJ (2006) Phase I trial of sorafenib and gemcitabine in advanced solid tumors with an expanded cohort in advanced pancreatic cancer. *Clin Cancer Res* **12:** 144–151

Solberg HE (1987) International Federation of Clinical Chemistry (IFCC). Approved recommendation (1986) on the theory of reference values. Part 1. The concept of reference values. *J Clin Chem Clin Biochem* **25:** 337–342

Takano S, Yoshitomi H, Togawa A, Sogawa K, Shida T, Kimura F, Shimizu H, Tomonaga T, Nomura F, Miyazaki M (2008) Apolipoprotein C-1 maintains cell survival by preventing from apoptosis in pancreatic cancer cells. *Oncogene* **27:** 2810–2822

Villanueva J, Lawlor K, Toledo-Crow R, Tempst P (2006a) Automated serum peptide profiling. *Nat Protco* **1:** 880–889

Villanueva J, Shaffer DR, Philip J, Chaparro CA, Erdjument-Bromage H, Olshen AB, Fleisher M, Lilja H, Brogi E, Boyd J, Sanchez-Carbayo M, Holland EC, Cordon-Cardo C, Scher HI, Tempst P (2006b) Differential exoprotease activities confer tumor-specific serum peptidome patterns. *J Clin Invest* **116:** 271–284

Zhang Z, Bast Jr RC, Yu Y, Li J, Sokoll LJ, Rai AJ, Rosenzweig JM, Cameron B, Wang YY, Meng XY, Berchuck A, Van Haaften-Day C, Hacker NF, de Bruijn HW, van der Zee AG, Jacobs IJ, Fung ET, Chan DW (2004) Three biomarkers identified from serum proteomic analysis for the detection of early stage ovarian cancer. *Cancer Res* **64:** 5882–5890

Radiotherapy and Oncology 96 (2010) 236–242

Contents lists available at ScienceDirect

Radiotherapy and Oncology

journal homepage: www.thegreenjournal.com

Particle beam radiotherapy

Compensatory enlargement of the liver after treatment of hepatocellular carcinoma with carbon ion radiotherapy – Relation to prognosis and liver function

Hiroshi Imada [a,b,*], Hirotoshi Kato [a], Shigeo Yasuda [a], Shigeru Yamada [a], Takeshi Yanagi [a], Ryusuke Hara [a], Riwa Kishimoto [a], Susumu Kandatsu [a], Shinichi Minohara [a], Jun-etsu Mizoe [a], Tadashi Kamada [a], Osamu Yokosuka [b], Hirohiko Tsujii [a]

[a] *Research Center for Charged Particle Therapy, National Institute of Radiological Sciences, Chiba, Japan;* [b] *Department of Medicine and Clinical Oncology, Graduate School of Medicine, Chiba University, Chiba, Japan*

ARTICLE INFO

Article history:
Received 30 December 2008
Received in revised form 3 December 2009
Accepted 18 March 2010
Available online 21 April 2010

Keywords:
Hepatocellular carcinoma
Radiotherapy
Carbon ion
Liver volume
Liver function

ABSTRACT

Background and purpose: To examine whether liver volume changes affect prognosis and hepatic function in patients treated with carbon ion radiotherapy (CIRT) for hepatocellular carcinoma (HCC).

Material and methods: Between April 1995 and March 2003, among the cases treated with CIRT, 43 patients with HCC limited to the right hepatic lobe were considered eligible for the study. The left lateral segment was defined as the non-irradiated region. Liver volume was measured using contrast CT at 0, 3, 6, and 12 months after CIRT. We examined serum albumin, prothrombin activity, and total bilirubin level as hepatic functional reserve.

Results: After CIRT, the non-irradiated region showed significant enlargement, and enlarged volume of this region 3 months after CIRT $\geqslant 50\ cm^3$ was a prognostic factor. The 5-year overall survival rates were 48.9% in the larger enlargement group (enlarged volume of non-irradiated region 3 months after CIRT $\geqslant 50\ cm^3$) and 29.4% in the smaller enlargement group (as above, $<50\ cm^3$). The larger enlargement group showed better hepatic functional reserve than the smaller enlargement group 12 months after CIRT.

Conclusions: This study suggests that compensatory enlargement in the non-irradiated liver after CIRT contributes to the improvement of prognosis.

Hepatocellular carcinoma (HCC) is one of the most common malignant tumors in the world and is the third-leading cause of death from cancer [1]. In Japan, its incidence is approximately 30 in 100,000 males and 10 in 100,000 females [2]. HCC is closely associated with hepatitis B and C, and the majority of patients with HCC have liver cirrhosis, a condition that limits treatment options. Surgical resection is the mainstay of curative treatment, but it is restricted to selected patients [3,4]. Radiofrequency ablation and other ablative techniques achieve excellent local control, but they are restricted to small HCC [5–7]. Transcatheter arterial chemoembolization is clinically useful [8–10], but a radical effect has not been proved in histopathologic studies [11,12]. There is an urgent need for more effective and less invasive treatment of HCC.

The previous role of radiotherapy for HCC was limited and unsatisfactory by poor hepatic tolerance to irradiation [13,14]. Technological advances have made it possible to deliver a higher dose of radiation to focal liver cancers accurately, reducing the risk of toxicity [15–17]. Proton beam therapy has appeared to be effective and safe for HCC, mainly because of its excellent dose distribution at the end of the beam path, called the Bragg peak [18,19]. Carbon ion beams also possess the Bragg peak, and they provide excellent dose localization to the target volume by specified beam modulations [20,21]. They have advantageous biological and physical properties that result in a higher cytocidal effect than those of photons and protons [22–27].

The history of the use of carbon ion radiotherapy (CIRT) for treating HCC goes back to 1995, when clinical trials were initiated at the National Institute of Radiological Sciences (NIRS). We have already reported that CIRT used for the treatment of HCC is safe and effective, and that it causes only minor liver damage [22,23]. Although atrophy of the irradiated region of the liver is observed after CIRT, the reason why liver function is retained after CIRT has not yet been investigated.

It has been reported that preoperative portal vein embolization in extended hepatectomy cases causes the remnant liver volume to increase and postoperative hepatic insufficiency to diminish [28,29]. Similarly, we wondered whether the same mechanism might apply to CIRT. Thus, as the region irradiated with CIRT showed atrophy and the non-irradiated region appeared to show

* Corresponding author at: Research Center for Charged Particle Therapy, National Institute of Radiological Sciences, 4-9-1, Anagawa, Inage-ku, Chiba 263-8555, Japan.
E-mail address: h_imada@nirs.go.jp (H. Imada).

0167-8140/$ - see front matter © 2010 Elsevier Ireland Ltd. All rights reserved.
doi:10.1016/j.radonc.2010.03.025

compensatory enlargement after CIRT, it was supposed that the compensatory enlargement had a contributory role in the retention of hepatic function. This hypothesis was investigated.

Materials and methods

Patients

CIRT for HCC was performed as a Phase I/II clinical trial from April 1995 through March 2001 with 110 patients, and as a Phase II clinical trial from April 2001 through March 2003 with 47 patients. The eligibility criteria for enrollment in these clinical trials were previously reported [22]. Prior to treatment, all patients gave their written informed consent in accordance with the Declaration of Helsinki. One hundred twenty-one of the total 157 had the tumor limited to the right lobe of the liver, 27 had the tumor limited to the left lobe, and 9 had the tumor in both right and left lobes.

Among the patients of this study, 43 met the following conditions: (1) treatment target tumor was limited to the right lobe of the liver, (2) left lateral segment was not irradiated, (3) no additional treatment was performed for hepatic lesions (local recurrence and/or recurrence in other loci) within 12 months after CIRT, and (4) abdominal contrast CT imaging was performed at our institute at 0, 3, 6 and 12 months after CIRT. Background data of the patients and tumors are presented in Table 1. The regions irradiated with more than 10% radiation dose were as follows: anterior, posterior and medial segments in 32 patients, anterior and posterior segments in 8, posterior segment in 2, and anterior and medial segments in 1.

Carbon ion radiotherapy

The carbon ion beam used for radiotherapy was generated from the heavy ion medical accelerator in Chiba developed by NIRS in 1993. The accelerator system and the biophysical characteristics of the carbon ion beam have been previously described [20,21,30]. For modulation of the Bragg peak of the beam to conform to the target volume, the beam lines in the treatment room are equipped with a pair of wobbler magnets, beam scatterers, ridge filters, multileaf collimators, and a compensation bolus. The irradiation fields were established with a three-dimensional therapy plan on the basis of 5-mm-thick CT images. The planning target volume was defined according to the shape of the tumor plus a 1.0–1.2 cm margin. To reproduce the target position accurately, a low-temperature thermoplastic sheet (Shellfitter, Kuraray, Osaka, Japan), a customized cradle (Moldcare, Alcare, Tokyo, Japan), and a respiratory gated irradiation system [31] were used in the CT planning and radiotherapy stages. The radiation field was confirmed and corrected by orthogonal fluoroscopy and radiography immediately before each treatment session.

Table 1
Patient and tumor characteristics.

	Total	Larger enlargement group	Smaller enlargement group	*P*
n	43	20	23	
Gender, n (%)				
Male	29 (67)	15 (75)	14 (61)	0.353
Female	14 (33)	5 (25)	9 (39)	
Age (years)				
Median	66	71.5	65	0.006
Range	45–83	46–81	45–83	
Child-Pugh classification, n (%)				
A	35 (81)	18 (90)	17 (74)	0.250
B	8 (19)	2 (10)	6 (26)	
Stage (UICC 5th), n (%)				
I	13 (32)	6 (27)	7 (36)	0.947
II	25 (54)	12 (59)	13 (50)	
IIIA	5 (14)	2 (14)	3 (14)	
Gross tumor volume (cm^3)				
Median	35.2	54.7	31.8	0.114
Range	4.6–861.9	15.6–861.9	4.6–211.2	
Planning target volume (cm^3)				
Median	190.5	242.9	149.0	0.019
Range	39.6–1466.4	70.3–1466.4	39.6–538	
Liver volume of irradiated site (cm^3), mean ± SD	756.6 ± 134.1	767.1 ± 138.1	747.5 ± 132.9	0.942
Liver volume of non-irradiated site (cm^3), mean ± SD	320.0 ± 166.3	317.2 ± 152.7	322.4 ± 180.6	0.715
Albumin (g/dl), mean ± SD	3.8 ± 0.4	3.9 ± 0.4	3.8 ± 0.4	0.659
Prothrombin activity (%), mean ± SD	77.2 ± 13.5	78.6 ± 11.4	76.0 ± 15.3	0.670
Total bilirubin (mg/dl), mean ± SD	1.0 ± 0.4	0.9 ± 0.3	1.1 ± 0.4	0.072
Platelet count ($\times 10^4/\mu l$), mean ± SD	11.8 ± 4.6	14.0 ± 4.3	9.9 ± 3.9	0.002
Number of tumors, n (%)				
1	36 (84)	19 (95)	17 (74)	0.100
2	7 (16)	1 (5)	6 (26)	
Irradiated segment, n (%)				
Anterior, posterior and medial	32	15	17	0.821
Anterior and posterior	8	4	4	
Posterior	2	1	1	
Anterior and medial	1	0	1	
Number of portals, n (%)				
2	36	16	20	0.687
3	7	4	3	

Abbreviations: UICC = International Union Against Cancer.
SD = standard deviation.

Table 2
Dose fractionation.

Total dose/ fractionation	Total ($n = 43$)	Larger enlargement group ($n = 20$)	Smaller enlargement group ($n = 23$)	BED ($\alpha/\beta = 10$)
49.5 GyE/15 fr	1	1	0	65.8
54.0 GyE/15 fr	1	0	1	73.4
60.0 GyE/15 fr	2	0	2	84.0
66.0 GyE/15 fr	2	1	1	95.0
72.0 GyE/15 fr	3	1	2	106.6
79.5 GyE/15 fr	1	0	1	121.6
54.0 GyE/12 fr	1	0	1	78.3
60.0 GyE/12 fr	3	2	1	90.0
66.0 GyE/12 fr	2	2	0	102.3
69.6 GyE/12 fr	4	1	3	110.0
48.0 GyE/8 fr	2	0	2	76.8
52.8 GyE/8 fr	7	3	4	87.6
52.8 GyE/4 fr	14	9	5	122.5

Abbreviations: BED = biological effective dose.

The dose was calculated for the target volume and any nearby critical structures and expressed in Gray equivalents (GyE = carbon physical dose [in Gray] × relative biologic effectiveness). Radiobiologic studies were performed in mice and in five human cell lines cultured *in vitro* to estimate the relative biologic effectiveness values relative to megavoltage photons. Irrespective of the size of the spread-out Bragg peak (SOBP), the relative biologic effectiveness value of carbon ions was estimated as 3.0 at the distal part of the SOBP, and ridge filters were designed to produce a physical dose gradient of the SOBP so that the biologic effect along the SOBP became uniform. This was based on the biologic response of human salivary gland tumor cells at a 10% survival level.

CIRT was given at a total dose range of 48.0–79.5 GyE in 4–15 fractions. Ten patients were treated at a total dose range of 49.5–79.5 GyE in 15 fractions, 10 at 54.0–69.6 GyE in 12 fractions, 9 at 48.0–52.8 GyE in 8 fractions, and 14 at 52.8 GyE in four fractions. CIRT was administered once a day, four fractions per a week, and one port was used in each session. Double-field geometry was used for CIRT in 36 patients; for the remaining seven patients, three-field geometry was used (Tables 1 and 2).

Measurement of liver volume

The left lateral segment of the liver was defined as the non-irradiated region, and the other segments as irradiated. The AZE Company Workstation VIRTUAL PLACE ADVANCE PLUS liver analysis software was used for measuring liver volume. Liver contours (both irradiated and non-irradiated regions) and contours of the target tumors to be treated were entered on each of the CT slices taken prior to treatment and at 3, 6 and 12 months after CIRT, and the volume of the liver in the irradiated region (excluding the target tumor volume) as well as that in the non-irradiated region were measured. Since hepatic cirrhosis is noted in most cases as the background disease, and to exclude any impact of right lobe atrophy and left lobe enlargement through natural processes, the evaluation period was limited to 12 months after treatment.

Survival and evaluation of liver function

Overall survival was measured from the starting date of treatment until the date of death from any cause. Disease-free survival was measured from the starting date of treatment to the time of either death due to disease or of the first clinical or radiographic evidence of systemic or regional disease recurrence. We investigated the relationships between survivals and enlargement volume of the non-irradiated region at 3 months after CIRT. Patients with 50 cm^3 or greater enlargement volume of the non-irradiated region at 3 months post-treatment were classified as the larger enlargement group, and those with less than 50 cm^3 enlargement as the smaller enlargement group. Serial changes in serum albumin, prothrombin activity, total bilirubin level, and platelet count were reviewed before and 12 months after treatment in the larger and smaller enlargement groups.

Statistical analysis

Statistical analyses were performed using SPSS version 12.0 (SPSS Inc., Chicago, IL). Results were reported as mean ± standard deviation. For continuous variables, non-parametric tests (Friedman test, Wilcoxon's signed *r* rank test, and Mann–Whitney *U* test) were used. For categorical data, chi-squared test or Fisher's exact test was used. Prognostic factor analyses were performed using the Cox proportional hazards regression model. The Kaplan–Meier method was used for calculation of survival rates, and survival curves were compared by log-rank test. Multivariate analyses of factors related to enlargement of the non-irradiated region at 3 months after CIRT were performed using logistic regression analyses. Statistical significance was considered if $P < 0.05$ (*P*-values from two-sided tests), but for multiple comparisons of liver volume, Bonferroni's inequality was used.

Table 3
Changes in liver volume.

	Before	3 months after	6 months after	12 months after
Total ($n = 43$)				
Irradiated region (cm^3)	756.6 ± 134.1	696.1 ± 229.1	632.9 ± 164.2	575.9 ± 145.7
Volume variation (cm^3) (%)	−60.5 ± 204.3 (−7.8 ± 28.1)	−123.7 ± 145.7 (−15.9 ± 19.0)	−180.7 ± 104.2 (−24.0 ± 13.7)	
Non-irradiated region (cm^3)	320.0 ± 166.3	379.4 ± 169.4	389.5 ± 177.5	390.4 ± 185.7
Volume variation (cm^3) (%)	59.4 ± 80.4 (25.3 ± 37.2)	69.5 ± 85.3 (28.7 ± 36.6)	70.4 ± 85.2 (27.0 ± 33.9)	
Larger enlargement group ($n = 20$)				
Irradiated region (cm^3)	767.1 ± 138.1	726.7 ± 294.5	662.8 ± 178.8	582.7 ± 149.3
Volume variation (cm^3) (%)	−40.4 ± 279.8 (−4.7 ± 39.1)	−104.3 ± 177.7 (−12.7 ± 23.8)	−184.4 ± 111.9 (−24.1 ± 15.3)	
Non-irradiated region (cm^3)	317.2 ± 152.7	438.1 ± 152.0	444.9 ± 165.0	441.9 ± 162.7
Volume variation (cm^3) (%)	120.9 ± 74.1 (47.7 ± 42.6)	127.7 ± 84.0 (50.3 ± 40.5)		
Smaller enlargement group ($n = 23$)				
Irradiated region (cm^3)	747.5 ± 132.9	669.4 ± 154.1	606.9 ± 149.4	570.0 ± 145.7
Volume variation (cm^3) (%)	−78.1 ± 106.6 (−10.4 ± 13.2)	−140.6 ± 112.3 (−18.7 ± 13.6)	−177.5 ± 99.4 (−24.0 ± 12.4)	
Non-irradiated region (cm^3)	322.4 ± 180.6	328.3 ± 170.2	341.3 ± 177.3	345.6 ± 196.1
Volume variation (cm^3)(%)	5.9 ± 34.0 (5.8 ± 15.2)	18.9 ± 45.2 (10.0 ± 18.8)	23.2 ± 60.1 (9.6 ± 20.6)	

Values are given as mean ± standard deviation.

Results

The changes with time in liver volume values are shown in Table 3. In all patients, the volume of the irradiated region decreased significantly and that of the non-irradiated region increased significantly by the Friedman test ($P < 0.001$, $P < 0.001$, respectively), with the difference over time in the irradiated region by multiple comparisons showing that significant differences existed between any two time-points ($P < 0.001$, each). In the non-irradiated region, comparisons showed that significant differences existed between before treatment and 3, 6, and 12 months after treatment ($P < 0.001$, $P < 0.001$, $P < 0.001$, respectively), but there were no significant differences between 3 and 6 months, 3 and 12 months, and 6 and 12 months ($P = 0.091$, $P = 0.084$, and $P = 0.599$, respectively). Comparing the time-related changes of the liver volume in terms of the larger and smaller enlargement groups, both of the two groups showed significant atrophy of the irradiated region ($P < 0.001$, $P < 0.001$, respectively) and significant enlargement of the non-irradiated region ($P < 0.001$, $P = 0.022$, respectively) (Fig. 1). Further, the enlarged volume of the non-irradiated region 3 months after CIRT $\geqslant 50\ cm^3$ was a prognostic factor (Table 4).

There were significant differences between the larger and smaller enlargement groups in overall survival rate and disease-free survival rate ($P = 0.030$, $P = 0.008$, respectively). Overall survival rates after 3 and 5 years were 80.0% (95% confidence interval [CI], 63–98) and 48.9% (95% CI, 27–71) in the larger enlargement group and 52.2% (95% CI, 32–73) and 29.4% (95% CI, 10–48) in the smaller enlargement group (Fig. 2a). Disease-free survival rates after 3 and 5 years were 50.0% (95% CI, 28–72) and 28.0% (95% CI, 7–49) in the larger enlargement group and 26.1% (95% CI, 8–44) and 0.0% (95% CI, 0–0) in the smaller enlargement group (Fig. 2b).

Table 5 shows the comparison of liver function between the two groups. Before treatment, there were no significant differences in serum albumin, prothrombin activity, and total bilirubin level between the two groups ($P = 0.659$, $P = 0.670$, and $P = 0.072$, respectively). Yet, 12 months after the treatment the larger enlargement group exhibited significantly higher serum albumin and prothrombin activity and lower total bilirubin levels than the smaller enlargement group ($P = 0.015$, $P = 0.002$, $P = 0.042$, respectively). As for platelet count, there were significant differences between the two groups before and after the treatment ($P = 0.002$, $P = 0.002$, respectively).

Univariate analysis showed that the planning target volume (PTV) and platelet count were significant factors for compensatory liver enlargement. Multivariate analysis showed only platelet count to be a significant factor (Table 6).

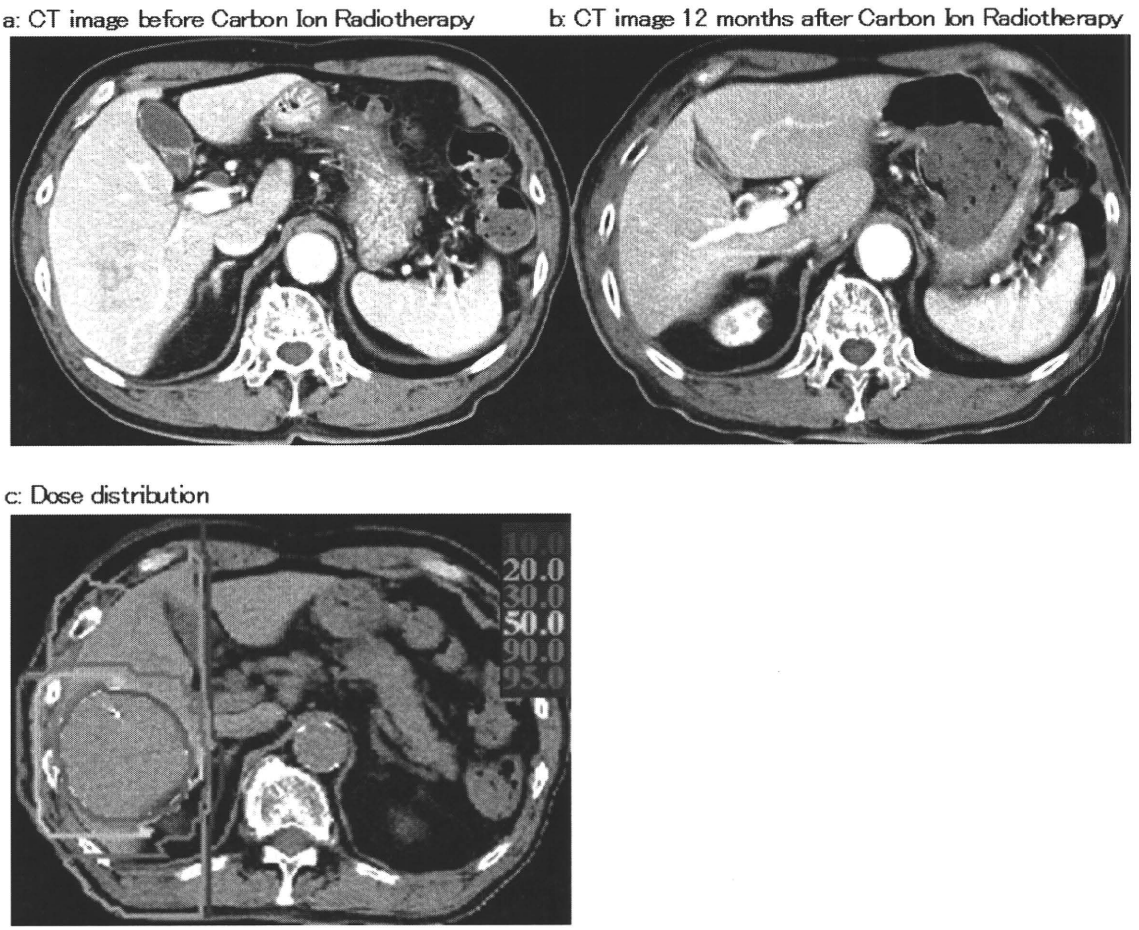

Fig. 1. CT images before and 12 months after carbon ion radiotherapy and dose distribution. CT image obtained in 81-year-old man from the larger enlargement group shows shrinkage of right hepatic lobe ($840.5\ cm^3 \rightarrow 739.0\ cm^3$) and enlargement of left lateral segment ($154.5\ cm^3 \rightarrow 266.4\ cm^3$). Hepatic function of this patient was retained. Serum albumin level before and 12 months after therapy was 4.5 and 4.0 g/dl, respectively. Prothrombin activity was 85.7% and 82.7%, respectively. Total bilirubin level was 0.7 and 0.7 mg/dl, respectively. Platelet count was 13.5×10^4 and $17.8 \times 10^4/\mu l$, respectively.

Table 4
Factors related to overall survival.

Factor	No. of patients	Univariate		Multivariate	
		Hazard ratio (95% CI)	*P*	Hazard ratio (95% CI)	*P*
Gender					
Male	29	1.00 (0.47–2.10)	0.994	0.55 (0.18–1.72)	0.305
Female	14				
Age (years)					
<65	15	1.12 (0.59–2.43)	0.614	1.82 (0.80–4.18)	0.155
⩾65	28				
Child-Pugh classification					
A	35	1.40 (0.63–3.10)	0.406	1.48 (0.45–4.85)	0.520
B	8				
Platelet count ($\times 10^4/\mu l$)					
<10	17	0.57 (0.29–1.15)	0.114	0.51 (0.20–1.33)	0.169
⩾10	26				
Enlargement volume of non-irradiated region at 3 months after CIRT (cm^3)					
<50	23	0.45 (0.22–0.94)	0.034	0.36 (0.15–0.88)	0.025
⩾50	20				
Planning target volume (cm^3)					
<200	24	0.78 (0.39–1.56)	0.489	1.51 (0.63–3.59)	0.357
⩾200	19				
Biological effective dose (α/β = 10)					
Low (65.8–95.0)	19	0.81 (0.41–1.62)	0.555	0.95 (0.41–2.20)	0.912
High (102.3–122.5)	24				
Number of tumors					
1	36	1.07 (0.44–2.61)	0.881	0.50 (0.16–1.54)	0.226
2	7				

Discussion

In the present study, we have shown that cases with irradiation of the right lobe of the liver develop enlargement of the left lateral segment by way of compensation after CIRT and that the compensatory enlargement is contributory to the improvement of prognosis.

Approximately 80% of all HCC patients have chronic liver disorders [3], which require effective and necessarily minimally invasive therapy of HCC. We have reported that CIRT appears safe and effective for patients with HCC [22,23]. However, the reason why liver function is retained despite atrophy of the irradiated region of the liver still remained to be investigated. Hemming et al. reported that preoperative portal vein embolization performed in extended hepatectomy cases caused enlargement of the remnant liver [28]. In other research studies, enlargement of the remnant liver has been shown to have the effect of improving liver function [32–34]. Moreover, after radiotherapy, veno-occlusive diseases of the liver occur, which, it is argued, are the cause of radiation-induced liver disease [35–37]. From the above, we wonder whether the same mechanism might hold true for CIRT.

In this study, we measured the volumes of the irradiated and non-irradiated regions using CT imaging. Heymsfield and associates first measured the volume of a cadaver's liver using CT in 1979, showing that the discrepancy between the volume measured by CT and that measured using the water replacement method was

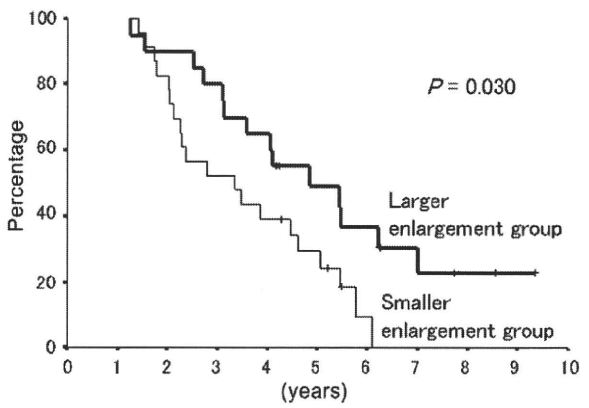

Fig. 2a. Survival rates of the larger and smaller enlargement groups. (a) Overall survival of the larger and smaller enlargement groups. Overall survival rates after 3 and 5 years were 80.0% (95% confidence interval [CI], 63–98) and 48.9% (95% CI, 27–71) in the larger enlargement group and 52.2% (95% CI, 32–73) and 29.4% (95% CI, 10–48) in the smaller enlargement group.

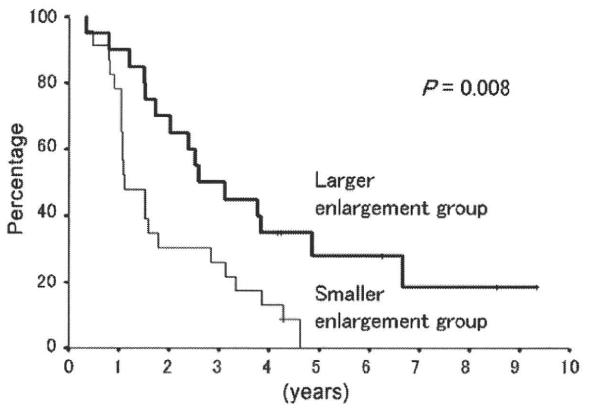

Fig. 2b. Survival rates of the larger and smaller enlargement groups. (b) Disease-free survival of the larger and smaller enlargement groups. Disease-free survival rates after 3 and 5 years were 50.0% (95% CI, 28–72) and 28.0% (95% CI, 7–49) in the larger enlargement group and 26.1% (95% CI, 8–44) and 0.0% (95% CI, 0–0) in the smaller enlargement group.

Table 5
Comparison of liver function.

	Before			12 months after		
	Larger enlargement group ($n = 20$)	Smaller enlargement group ($n = 23$)	P	Larger enlargement group ($n = 20$)	Smaller enlargement group ($n = 23$)	P
Albumin (g/dl)	3.9 ± 0.4	3.8 ± 0.4	0.659	3.9 ± 0.3	3.7 ± 0.4	0.015
Prothrombin activity (%)	78.6 ± 11.4	76.0 ± 15.3	0.670	81.9 ± 9.3	69.7 ± 11.9	0.002
Total bilirubin (mg/dl)	0.9 ± 0.3	1.1 ± 0.4	0.072	0.9 ± 0.5	1.1 ± 0.4	0.042
Platelet count ($\times 10^4$/μl)	14.0 ± 4.3	9.9 ± 3.9	0.002	14.6 ± 7.9	8.5 ± 3.4	0.002

Values are given as mean ± standard deviation.

Table 6
Factors related to compensatory enlargement.

Factor	No. of patients	Univariate P	Multivariate P	Hazard ratio	95% Confidence interval
Planning target volume (PTV) (cm^3)					
<200	24	0.013	0.147	2.92	0.69–12.46
⩾200	19				
Platelet count ($\times 10^4/\mu l$)					
<10	17	0.004	0.028	5.85	1.21–28.31
⩾10	26				
Biological effective dose (BED) ($\alpha/\beta = 10$)					
Low (65.8–95.0)	19	0.261	0.479	1.67	0.40–6.94
High (102.3–122.5)	24				

within 5% [38]. In 1981, Moss et al. also measured liver volume using CT, confirming the conclusion of Heymsfield et al. [39]. Many studies have reported that the difference between CT-measured liver volume and the actual liver volume is minor [38–40]. In our study, the volume of the left lateral segment was 320.0 ± 166.3 cm^3 (Table 3). Zhou et al. measured the volume of 113 hepatic lobes using CT. They reported average volumes of the left lateral segment of 313.2 ± 105.1 and 282.2 ± 136.2 cm^3 in Child-Pugh class A and B patients, respectively [41]. These results generally resemble ours, lending support to the accuracy and reliability of our measuring method.

It is difficult to distinguish strictly the irradiated and non-irradiated portions, and therefore in this study we defined the left lateral segment of the liver as the non-irradiated region, and the other segments as irradiated. In 11 of 43 patients, the region considered as irradiated was larger than the region really receiving radiation. We cannot examine whether the non-irradiated portions of the right lobes enlarge or not because it is difficult to distinguish the irradiated and non-irradiated portions of the right lobe. The volumes of the irradiated part of the liver measured at 0, 3, 6, and 12 months after treatment, respectively, did show significant differences. With the lapse of time, the measurement values decreased significantly. In contrast, the liver volumes of the non-irradiated part increased at 3 months post-treatment on a significant scale compared to before the treatment. From then on, no more significant increases were observed. These data demonstrate that the enlargement of the non-irradiated region is not a matter of the natural course associated with chronic liver disorders, but rather results as compensation for the CIRT-caused atrophy of the liver.

We divided the subjects into two groups according to compensatory enlargement liver volume of more or less than 50 cm^3 because enlarged volume of the non-irradiated region 3 months after CIRT ⩾50 cm^3 was a prognostic factor. In terms of liver function, many complex methods for estimating liver functional reserve have been advocated, including tests that measure liver metabolic activity such as ICG clearance, galactose elimination, and aminopyrine clearance [42]. However, it was demonstrated that either one of Child classification [43] or Okuda staging [44] is highly predictive for outcome [45]. Serum albumin, prothrombin activity, and total bilirubin level are the serum items of the Child-Pugh score, which is the index of hepatic functional reserve. Therefore, Serial changes in these items were reviewed as hepatic functional reserve before and 12 months after treatment in the two groups. There were no significant differences in them before the treatment, but at 12 months after, the larger enlargement group remained significantly more favorable than the smaller enlargement group. On the other hand, the extent of atrophy of the irradiated regions was found to be significantly similar in the two groups. These data indicate the possibility that the compensatory enlargement, taking place in the non-irradiated region of the liver after CIRT, affect hepatic functional reserve. It was suggested that better disease-free survival and hepatic functional reserve contributed to improvement of overall survival.

We investigated PTV, platelet count, and biological effective dose (BED) as indicators of enlargement of the non-irradiated region at 3 months after CIRT. PTV and platelet count were selected on the basis of their significant differences between the larger and smaller enlargement groups. In our study, it was difficult to compare the differences of total dose and fractionations because of their various combinations. Then, although it has not been confirmed that BED is adaptable to CIRT, we tried to calculate BED for every fractionation by L/Q model [46], adding it to the variables. The difference in mean age between the two groups was thought not to be related to the compensatory enlargement of the liver after CIRT, based on the self-evident discrepancy between age and the enlargement volume, i.e., the higher the age, the larger the volume. Therefore, we excluded age from the analysis of the indicators of compensatory enlargement of the non-irradiated liver. Our data demonstrated platelet count to be the major factor of compensatory enlargement of the non-irradiated liver, and it is known that platelet count decreases in parallel with the grade of chronic liver disease [47]. Thus, we intend to investigate the relationship between liver fibrosis and compensatory enlargement of the liver in future studies.

Considering the limitations of this study, we must first point out the nature of the investigation as a retrospective one. Secondly, the subjects were restricted to cases in which target tumors were located in the right lobe of the liver. Thirdly, we did not utilize any biochemical or molecular biological method.

It was demonstrated that the non-irradiated region of the liver enlarged compensatively until 3 months after CIRT and that the enlarged volume of this region 3 months after CIRT ⩾50 cm^3 was a prognostic factor. We can conclude that compensatory enlargement of the non-irradiated liver contributes to the improvement of prognosis.

Conflict of interest statement

Any actual or potential conflicts of interest do not exist.

Acknowledgments

This study was supported by the Research Project with Heavy Ions of the National Institute of Radiological Sciences in Japan. We are grateful to members of the National Institute of Radiological Sciences. We are indebted to Dr. Gen Kobashi and Dr. Kaori Ohta for statistical support.

References

[1] Bosch FX, Ribes J, Borras J. Epidemiology of primary liver cancer. Semin Liver Dis 1999;19:271–85.
[2] Marugame T, Matsuda T, Kamo K, et al. Cancer incidence and incidence rates in Japan in 2001 based on the data from 10 population-based cancer registries. Jpn J Clin Oncol 2007;37:884–91.
[3] Ikai I, Arii S, Okazaki M, et al. Report of the 17th Nationwide Follow-up Survey of Primary Liver Cancer in Japan. Hepatol Res 2007;37:676–91.
[4] Mulcahy MF. Management of hepatocellular cancer. Curr Treat Options Oncol 2005;6:423–35.
[5] Kuvshinoff BW, Ota DM. Radiofrequency ablation of liver tumors: influence of technique and tumor size. Surgery 2002;132:605–11.
[6] Shiina S, Teratani T, Obi S, et al. A randomized controlled trial of radiofrequency ablation with ethanol injection for small hepatocellular carcinoma. Gastroenterology 2005;129:122–30.
[7] Sato M, Watanabe Y, Ueda S, et al. Microwave coagulation therapy for hepatocellular carcinoma. Gastroenterology 1996;110:1507–14.
[8] Camma C, Schepis F, Orlando A, et al. Transarterial chemoembolization for unresectable hepatocellular carcinoma: meta-analysis of randomized controlled trials. Radiology 2002;224:47–54.
[9] Lo CM, Ngan H, Tso WK, et al. Randomized controlled trial of transarterial lipiodol chemoembolization for unresectable hepatocellular carcinoma. Hepatology 2002;35:1164–71.
[10] Llovet JM, Real MI, Montana X, et al. Arterial embolization or chemoembolization versus symptomatic treatment in patients with unresectable hepatocellular carcinoma: a randomized controlled trial. Lancet 2002;359:1734–9.
[11] Higuchi T, Kikuchi M, Okazaki M. Hepatocellular carcinoma after transcatheter hepatic arterial embolization. A histopathologic study of 84 resected cases. Cancer 1994;73:2259–67.
[12] Adachi E, Matsumata T, Nishizaki T, Hashimoto H, Tsuneyoshi M, Sugimachi K. Effects of preoperative transcatheter hepatic arterial chemoembolization for hepatocellular carcinoma. The relationship between postoperative course and tumor necrosis. Cancer 1993;72:3593–8.
[13] Phillips R, Murikami K. Preliminary neoplasms of the liver. Results of radiation therapy. Cancer 1960;13:714–20.
[14] Stillwagon GB, Order SE, Guse C, et al. 194 hepatocellular cancers treated by radiation and chemotherapy combinations: toxicity and response: a Radiation Therapy Oncology Group study. Int J Radiat Oncol Biol Phys 1989;17:1223–9.
[15] Zhao JD, Xu ZY, Zhu J, et al. Application of active breathing control in 3-dimensional conformal radiation therapy for hepatocellular carcinoma: the feasibility and benefit. Radiother Oncol 2008;87:439–44.
[16] Toya R, Murakami R, Baba Y, et al. Conformal radiation therapy for portal vein tumor thrombosis of hepatocellular carcinoma. Radiother Oncol 2007;84:266–71.
[17] Robertson JM, Lawrence TS, Dworzanin LM, et al. Treatment of primary hepatobiliary cancers with conformal radiation therapy and regional chemotherapy. J Clin Oncol 1993;11:1286–93.
[18] Suit HD, Goitein M, Munzenrider J, et al. Increased efficacy of radiation therapy by use of proton beam. Strahlenther Onkol 1990;166:40–4.
[19] Matsuzaki Y, Osuga T, Saito Y, et al. A new, effective, and safe therapeutic option using proton irradiation for hepatocellular carcinoma. Gastroenterology 1994;106:1032–41.
[20] Kanai T, Endo M, Minohara S, et al. Biophysical characteristics of HIMAC clinical irradiation system for heavy-ion radiation therapy. Int J Radiat Oncol Biol Phys 1999;44:201–10.
[21] Kanai T, Furusawa Y, Fukutsu K, Itsukaichi H, Eguchi-Kasai K, Ohara H. Irradiation of mixed beam and design of spread-out Bragg peak for heavy-ion radiotherapy. Radiat Res 1997;147:78–85.
[22] Kato H, Tsujii H, Miyamoto T, et al. Results of the first prospective study of carbon ion radiotherapy for hepatocellular carcinoma with liver cirrhosis. Int J Radiat Oncol Biol Phys 2004;59:1468–76.
[23] Kato H, Yamada S, Yasuda S, et al. Phase II study of short-course carbon ion radiotherapy (52.8GyE/4-fraction/1-week) for hepatocellular carcinoma. Hepatology 2005;42(Suppl. 1):381A.
[24] Blakely EA, Ngo FQH, Curtis SB, et al. Heavy ion radiobiology: cellular studies. Adv Radiat Biol 1984;11:295–378.
[25] Castro JR. Future research strategy for heavy ion radiotherapy. In: Kogelnih HD, editor. Progress in radio-oncology. Bologna: Monduzzi Editore; 1995. p. 643–8.
[26] Tsujii H, Morita S, Miyamoto T, et al. Preliminary results of phase I/II carbon ion therapy. J Brachyther Int 1997;13:1–8.
[27] Suzuki M, Kase Y, Yamaguchi H, Kanai T, Ando K. Relative biological effectiveness for cell-killing effect on various human cell lines irradiated with heavy-ion medical accelerator in Chiba (HIMAC) carbon-ion beams. Int J Radiat Oncol Biol Phys 2000;48:241–50.
[28] Hemming AW, Reed AI, Howard RJ, et al. Preoperative portal vein embolization for extended hepatectomy. Ann Surg 2003;237:686–91.
[29] Abulkhir A, Limongelli P, Healey AJ, et al. Preoperative portal vein embolization for major liver resection: a meta-analysis. Ann Surg 2008;247:49–57.
[30] Sato K, Yamada H, Ogawa K, et al. Performance of HIMAC. Nucl Phys 1995;A588:229–34.
[31] Minohara S, Kanai T, Endo M, Noda K, Kanazawa M. Respiratory gated irradiation system for heavy-ion radiotherapy. Int J Radiat Oncol Biol Phys 2000;47:1097–103.
[32] Kubo S, Shiomi S, Tanaka H, et al. Evaluation of the effect of portal vein embolization on liver function by (99m)tc-galactosyl human serum albumin scintigraphy. J Surg Res 2002;107:113–8.
[33] Kudo M, Todo A, Ikekubo K, Yamamoto K, Vera DR, Standalnik RC. Quantitative assessment of hepatocellular function through in vivo radioreceptor imaging with technetium 99m galactosyl human serum albumin. Hepatology 1993;17:814–9.
[34] Vera DR, Topcu SJ, Stadalnik RC. In vitro quantification of asialoglycoprotein receptor density from human hepatic microsamples. Methods Enzymol 1994;247:394–402.
[35] Reed Jr GB, Cox Jr AJ. The human liver after radiation injury. A form of veno-occlusive disease. Am J Pathol 1966;48:597–611.
[36] Lawrence TS, Robertson JM, Anscher MS, Jirtle RL, Ensminger WD, Fajardo LF. Hepatic toxicity resulting from cancer treatment. Int J Radiat Oncol Biol Phys 1995;31:1237–48.
[37] Cheng JC, Wu JK, Huang CM, et al. Radiation-induced liver disease after radiotherapy for hepatocellular carcinoma: clinical manifestation and dosimetric description. Radiother Oncol 2002;63:41–5.
[38] Heymsfield SB, Fulenwider T, Nordlinger B, Barlow R, Sones P, Kutner M. Accurate measurement of liver, kidney, and spleen volume and mass by computerized axial tomography. Ann Intern Med 1979;90:185–7.
[39] Moss AA, Friedman MA, Brito AC. Determination of liver, kidney, and spleen volumes by computed tomography: an experimental study in dogs. J Comput Assist Tomogr 1981;5:12–4.
[40] Sakamoto S, Uemoto S, Uryuhara K, et al. Graft size assessment and analysis of donors for living donor liver transplantation using right lobe. Transplantation 2001;71:1407–13.
[41] Zhou XP, Lu T, Wei YG, Chen XZ. Liver volume variation in patients with virus-induced cirrhosis: findings on MDCT. AJR Am J Roentgenol 2007;189:W153–159.
[42] Friedman LS, Martin P, Santiago JM. Liver function tests and the objective evaluation of the patient with liver disease. In: Zakim D, Boyer TD, editors. Hepatology. Philadelphia: WB Saunders; 1996. p. 791–833.
[43] Wants GE, Payne MA. Experience with portacaval shunt for portal hypertension. N Engl J Med 1961;265:721–8.
[44] Okuda K, Ohtsuki T, Obata H, et al. Natural history of hepatocellular carcinoma and prognosis in relation to treatment. Cancer 1985;56:918–28.
[45] Fong Y, Sun RL, Jarnagin W, et al. An analysis of 412 cases of hepatocellular carcinoma at a western center. Ann Surg 1999;229:790–9.
[46] Lee SP, Leu MY, Smathers JB, et al. Biologically effective dose distribution based on the linear quadratic model and its clinical relevance. Int J Radiat Oncol Biol Phys 1995;33:375–89.
[47] Karasu Z, Tekin F, Ersoz G, et al. Liver fibrosis is associated with decreased peripheral count in patients with chronic hepatitis B and C. Dig Dis Sci 2007;52:1535–9.

Research Article

EASL EUROPEAN ASSOCIATION FOR THE STUDY OF THE LIVER | JOURNAL OF HEPATOLOGY

The polycomb group gene product Ezh2 regulates proliferation and differentiation of murine hepatic stem/progenitor cells

Ryutaro Aoki[1,2,†], Tetsuhiro Chiba[1,2,3,†], Satoru Miyagi[1], Masamitsu Negishi[1], Takaaki Konuma[1], Hideki Taniguchi[4], Makoto Ogawa[2], Osamu Yokosuka[2], Atsushi Iwama[1,3,*]

[1]*Department of Cellular and Molecular Medicine, Graduate School of Medicine, Chiba University, 1-8-1 Inohana, Chuo-ku, Chiba 260-8670, Japan;* [2]*Department of Medicine and Clinical Oncology, Graduate School of Medicine, Chiba University, 1-8-1 Inohana, Chuo-ku, Chiba 260-8670, Japan;* [3]*JST, CREST, Sanbancho, Chiyoda-ku, Tokyo 102-0075, Japan;* [4]*Department of Regenerative Medicine, Graduate School of Medicine, Yokohama City University, 3-9 Fukuura, Kanazawa-ku, Kanagawa 236-0004, Japan*

Background & Aims: Polycomb group proteins initiate and maintain gene silencing through chromatin modifications and contribute to the maintenance of self-renewal in a variety of stem cells. Among polycomb repressive complexes (PRCs), PRC2 initiates gene silencing by methylating histone H3 lysine 27, and PRC1 maintains gene silencing through mono-ubiquitination of histone H2A lysine 119. We have previously shown that Bmi1, a core component of PRC1, tightly regulates the self-renewal of hepatic stem/progenitor cells.

Methods: In this study, we conducted lentivirus-mediated knockdown of *Ezh2* to characterise the function of Ezh2, a major component of PRC2, in hepatic stem/progenitor cells.

Results: Loss of *Ezh2* function in embryonic murine hepatic stem/progenitor cells severely impaired proliferation and self-renewal capability. This effect was more prominent than that of *Bmi1*-knockdown and was partially abrogated by the deletion of both *Ink4a* and *Arf*, major targets of PRC1 and PRC2. Importantly, *Ezh2*-knockdown but not *Bmi1*-knockdown promoted the differentiation and terminal maturation of hepatocytes, followed by the up-regulation of several transcriptional regulators of hepatocyte differentiation.

Conclusions: Our findings indicate that Ezh2 plays an essential role in the maintenance of both the proliferative and self-renewal capacity of hepatic stem/progenitor cells and the full execution of their differentiation.

Keywords: Hepatic stem/progenitor cells; Ezh2; Bmi1; Ink4a/Arf; Self-renewal; Differentiation.

Received 18 September 2009; received in revised form 12 January 2010; accepted 14 January 2010; available online 24 March 2010

* Corresponding author. Address: Department of Cellular and Molecular Medicine, Graduate School of Medicine, Chiba University, 1-8-1 Inohana, Chuo-ku, Chiba 260-8670, Japan. Tel.: +81 43 2262187; fax: +81 43 2262191.

E-mail address: aiwama@faculty.chiba-u.jp (A. Iwama).

† These authors contributed equally to this work.

Abbreviations: PcG, polycomb group; PRC, polycomb repressive complex; H3K27, histone H3 at lysine 27; HCC, hepatocellular carcinoma; ED, embryonic day; EHS, Engelbreth–Holm–Swarm; OSM, oncostatin M; TNF, tumour necrosis factor; shRNA, short-hairpin RNA; ERP, enhanced red fluorescence protein; ChIP, chromatin immunoprecipitation; EGFP, enhanced green fluorescence protein; Alb, albumin; CK, cytokeratin; Epcam, epithelial cell adhesion molecule; ELISA, enzyme-linked immunosorbent assay; Gata1, GATA binding protein 1; TAT, tyrosine aminotransferase; G6P, glucose-6-phosphatase; PAS, periodic acid-Schiff; Itgb, integrin β; ES, embryonic stem; Hnf, hepatocyte nuclear factor; Cebp, CCAAT/enhancer binding protein.

Introduction

Stem cells are generally defined as self-renewing cell populations that can differentiate into multiple distinct cell types. Liver has an enormous capacity to regenerate after injury, although the mechanism of hepatic regeneration differs depending on the proliferation of pre-existing hepatocytes, homing of bone marrow cells, and proliferation and differentiation of hepatic stem cells [1]. In the developing murine liver, endodermal-derived hepatoblasts or hepatic stem/progenitor cells differentiate into hepatocytes and cholangiocytes [1]. Although hepatic stem/progenitor cells have been successfully identified in murine foetal liver [2,3], the molecular pathways regulating the self-renewal and differentiation of these cells are poorly understood.

Polycomb group (PcG) proteins form multiprotein complexes that play important roles in maintaining the transcriptional repression of target genes. Although PcG genes are best known for their role in maintaining the repression of *Hox* genes during development, they have been implicated in stem cell self-renewal and differentiation [4]. The PcG gene family members form two major distinct PcG complexes: one complex, known as polycomb repressive complex (PRC) 1, is composed of Ring1a/1b, Mph1, and Bmi1 or Mel18, and the other complex, PRC2, is composed of Eed, Suz12, and Ezh2. Ezh2 is a PcG protein homologous to *Drosophila* enhancer of zeste, a histone methyltransferase associated with transcriptional repression. Ezh2 has a SET domain that is typical of histone methyltransferases, and it catalyses the addition of methyl groups to histone H3 at lysine 27 (H3K27). In many cases, the methylation of H3K27 by Ezh2 results in the recruitment of PRC1, and the two PRCs cooperate in gene silencing [4]. Notably, expression of EZH2 together with BMI1 is reportedly associated with the progression and aggressiveness of hepatocellular carcinoma (HCC), and *EZH2*-knockdown inhibits the growth of cul-

tured human HCC cell lines [5]. We previously reported that Bmi1 enhances the self-renewal capacity of hepatic stem/progenitor cells and drives cancer initiation [6]. However, the role of Ezh2 in the hepatic stem cell system remains to be clarified.

In this study, we investigated the function of Ezh2 in foetal liver Dlk$^+$ hepatic stem/progenitor cells by knocking down *Ezh2* using lentivirus-mediated stable shRNA expression. *Ezh2*-knockdown profoundly inhibited the proliferation of Dlk$^+$ hepatic stem/progenitor cells and promoted differentiation into hepatocytes. These findings provide the first evidence of an essential role for Ezh2 in the homeostasis of the hepatic stem cell system.

Materials and methods

Mice

Pregnant C57BL/6 mice were purchased from Japan SLC (Hamamatsu, Japan). *Ink4a–Arf*$^{+/-}$ mice (Strain code 01XB1) obtained from Mouse Models of Human Cancers Consortium in NCI-Frederick (Frederick, MD, USA) were bred and maintained in accordance with our institutional guidelines for the use of laboratory animals.

Purification and culture of Dlk$^+$ cells

Dlk$^+$ cells were prepared from liver cell suspensions of embryonic day (ED) 14.5 foetal livers as described previously [2,3]. Briefly, cells were stained with rat anti-mouse Dlk monoclonal antibody (MBL, Nagoya, Japan) followed by anti-rat IgG-conjugated magnetic beads. Dlk$^+$ cells were purified by passage through cell separation columns in a magnetic field (Miltenyi Biotec, Bergisch Gladbach, Germany). They were plated at 1×10^3 cells/well on collagen type IV-coated 6-well plates (Becton Dickinson, Franklin lakes, NJ, USA) and cultured as described elsewhere [2,3]. Colony assays were performed in at least three independent triplicate experiments. To evaluate the potential to differentiate into hepatocytes, Dlk$^+$ cells were placed on an Engelbreth–Holm–Swarm (EHS) gel (Becton–Dickinson) in the presence of oncostatin M (OSM, R&D Systems, Minneapolis, MN, USA) [7]. Collagen type I gel culture (Nitta Gelatin, Osaka, Japan) in the presence of tumour necrosis factor (TNF)-α (Peprotech, Rocky Hill, NJ, USA) was also conducted to examine the ability to differentiate into cholangiocytes [8].

Viral production and transduction

Lentiviral vectors (CS-H1-shRNA-EF-1α-EGFP) expressing short-hairpin RNAs (shRNAs) against murine *Ezh2* (target sequence: sh-*Ezh2*-1, 5′-GGAAAGAACT-GAAACCTTA-3′; sh-*Ezh2*-2, 5′-GGTAAATGCTCTTGGTCAA-3′) were constructed. Lentiviral vectors (CS-H1-shRNA-EF-1α-EGFP) expressing shRNAs against *Bmi1* and *luciferase* were also used [6]. A lentiviral vector carrying enhanced red fluorescent protein (ERP) (CS-H1-shRNA-RfA-ERP) expressing shRNA against *Bmi1* was also constructed for the double knockdown of *Ezh2* and *Bmi1*. Recombinant lentiviruses were produced as described previously [6]. Purified cells were transduced with indicated viruses 12–18 h after pre-incubation.

Chromatin immunoprecipitation

Chromatin immunoprecipitation (ChIP) was performed as reported previously [9]. Briefly, cross-linked chromatin was sonicated into 200- to 500-bp fragments. The chromatin was immunoprecipitated using anti-Ezh2 (clone AC22, a gift from Dr. Kristian Helin) and anti-H3K27me3 (Millipore, Bedford, MA, USA) antibodies. Normal mouse IgG was used as a negative control. Quantitative PCR was conducted using SYBR Premix Ex Taq II (Takara Bio, Otsu, Japan). Primer sequences are listed in Supplementary Table 1 [10].

Statistics

Data are presented as the means ± SEM. Statistical differences were analysed using the Mann–Whitney *U* test. *p* values less than 0.05 were considered significant.

Results

Basal expression of Ezh2 and stable knockdown of Ezh2 in hepatic stem/progenitor cells

We first analysed the mRNA expression of *Ezh2* in hepatic stem/progenitor cells, which are enriched in the Dlk$^+$ cell fraction [2,3] in ED14.5 foetal liver. Haematopoietic cells were excluded by gating the CD45$^-$Ter119$^-$ cell fraction, and liver cells were divided into the Dlk$^+$ hepatic stem/progenitor fraction and the Dlk$^-$ non-stem/progenitor fraction. *Ezh2* expression was readily detected in both fractions, but quantitative RT-PCR and western blot analyses revealed a higher level of *Ezh2* expression in the Dlk$^+$ than the Dlk$^-$ fraction (Fig. 1A and B).

To investigate the function of Ezh2 in Dlk$^+$ hepatic stem/progenitor cells, we used lentivirus-mediated *Ezh2*-knockdown. Dlk$^+$ cells prepared from ED14.5 wild-type foetal livers were infected with sh-*Ezh2* viruses and allowed to propagate for 5 days. Flow-cytometric analyses revealed that the majority (more than 90%) of cells were positive for enhanced green fluorescent protein (EGFP), a marker of lentiviral integration (Fig. 1C). We compared the effect of the two shRNAs against *Ezh2* (sh-*Ezh2*-1 and sh-*Ezh2*-2) by real-time RT-PCR and western blot analyses. Real-time RT-PCR showed that the level of endogenous Ezh2 was markedly reduced in cells infected with lentivirus expressing shRNA against *Ezh2* compared with the control cells expressing shRNA against *luciferase* (sh-*Luc*) at multiple time points (Fig. 1D). Both shRNA severely reduced Ezh2 expression, although sh-*Ezh2*-2 was less effective than sh-*Ezh2*-1 (Fig. 1D). Concordant with this, the western blot analysis of cells at day 5 of culture showed that sh-*Ezh2*-1 was more effective in knocking down *Ezh2* than sh-*Ezh2*-2 (Fig. 1E). Therefore, we mainly used sh-*Ezh2*-1 in the following experiments, but we also obtained very similar results with sh-*Ezh2*-2 (Fig. 2C, D and data not shown).

Impaired proliferation and self-renewal of Dlk$^+$ cells following Ezh2-knockdown

It has been reported that approximately 15% of purified Dlk$^+$ cells gave rise to colonies at day 5 of culture. Among them, Dlk$^+$ cells, with the ability to form large colonies consisting of more than 100 cells at day 5 of culture, possess the properties of hepatic stem/progenitor cells. Because Dlk$^+$ cells produce a large number of Dlk$^-$ progeny, the proportion of Dlk$^+$ cells declines to less than 1% at day 5 of culture. Nonetheless, Dlk$^+$ cells in culture retain clonogenic activity [2,3]. Corresponding to these reports, almost 15% of Dlk$^+$ cells gave rise to colonies, which included a significant number of large colonies, while Dlk$^-$ cells scarcely gave rise to colonies, and no Dlk$^-$ cells generated large colonies at day 5 of culture (Fig. 2A). Next, we performed loss-of-function assays of *Ezh2* and/or *Bmi1* in Dlk$^+$ cells. Knockdown efficiencies were confirmed by western blot (Figs. 1E and 2B). *Ezh2*-knockdown modestly decreased the total number of colonies formed at day 5 of culture (Fig. 2C). By contrast, the number of large colonies derived from *Ezh2*-knockdown Dlk$^+$ cells was significantly decreased compared with the control, and most of the *Ezh2*-knockdown cells did not proliferate beyond 14 days (Fig. 2D). The effect of *Bmi1*-knockdown was milder than that of *Ezh2*-knockdown, and double knockdown of *Ezh2* and *Bmi1* had a limited advantage over single knockdown of *Ezh2* in inhibiting the proliferation of Dlk$^+$ cells